

A Technical and Economic Analysis of an Innovative Two-Step Absorption System for Utilizing Low-Temperature Geothermal Resources to Condition Commercial Buildings



Draft. Not for public release.

Xiaobing Liu
Zhiyao Yang
Kyle R. Gluesenkamp
Ayyoub M. Momen

December 2015

DOCUMENT AVAILABILITY

Reports produced after January 1, 1996, are generally available free via US Department of Energy (DOE) SciTech Connect.

Website <http://www.osti.gov/scitech/>

Reports produced before January 1, 1996, may be purchased by members of the public from the following source:

National Technical Information Service
5285 Port Royal Road
Springfield, VA 22161
Telephone 703-605-6000 (1-800-553-6847)
TDD 703-487-4639
Fax 703-605-6900
E-mail info@ntis.gov
Website <http://www.ntis.gov/help/ordermethods.aspx>

Reports are available to DOE employees, DOE contractors, Energy Technology Data Exchange representatives, and International Nuclear Information System representatives from the following source:

Office of Scientific and Technical Information
PO Box 62
Oak Ridge, TN 37831
Telephone 865-576-8401
Fax 865-576-5728
E-mail reports@osti.gov
Website <http://www.osti.gov/contact.html>

This report was prepared as an account of work sponsored by an agency of the United States Government. Neither the United States Government nor any agency thereof, nor any of their employees, makes any warranty, express or implied, or assumes any legal liability or responsibility for the accuracy, completeness, or usefulness of any information, apparatus, product, or process disclosed, or represents that its use would not infringe privately owned rights. Reference herein to any specific commercial product, process, or service by trade name, trademark, manufacturer, or otherwise, does not necessarily constitute or imply its endorsement, recommendation, or favoring by the United States Government or any agency thereof. The views and opinions of authors expressed herein do not necessarily state or reflect those of the United States Government or any agency thereof.

Energy and Transportation Science Division

**A TECHNICAL AND ECONOMIC ANALYSIS OF AN INNOVATIVE TWO-STEP
ABSORPTION SYSTEM FOR UTILIZING LOW-TEMPERATURE GEOTHERMAL
RESOURCES TO CONDITION COMMERCIAL BUILDINGS**

Xiaobing Liu
Zhiyao Yang
Kyle R. Gluesenkamp
Ayyoub M. Momen

Date Published: December 2015

Prepared by
OAK RIDGE NATIONAL LABORATORY
Oak Ridge, TN 37831-6283
managed by
UT-BATTELLE, LLC
for the
US DEPARTMENT OF ENERGY
under contract DE-AC05-00OR22725

CONTENTS

LIST OF FIGURES	v
LIST OF TABLES	vii
ABBREVIATED TERMS	ix
EXECUTIVE SUMMARY	xi
1. INTRODUCTION	1
2. OVERVIEW OF AVAILABLE LOW-TEMPERATURE GEOTHERMAL RESOURCES IN THE UNITED STATES	4
2.1 COPRODUCED WATER	4
2.2 GEOTHERMAL DIRECT USE	7
3. TWO-STEP GEOTHERMAL ABSORPTION COOLING SYSTEM	10
3.1 TARGET BUILDINGS	10
3.2 SELECTION OF WORKING FLUID PAIR.....	11
3.3 DESIGN SPECIFICATION OF A 900 TON TWO-STEP GEOTHERMAL ABSORPTION CHILLER.....	14
3.4 TECHNICAL CHALLENGES FOR TWO-STEP ABSORPTION	17
3.4.1 Minimize Amount of Working Fluid	17
3.4.2 Prevent Air Infiltration.....	17
3.4.3 Maintain Quality of Working Fluid	18
4. ECONOMIC ANALYSIS	19
4.1 BASELINE COOLING SYSTEM.....	20
4.1.1 Initial Cost.....	21
4.1.2 Operating Cost	21
4.2 TSGA SYSTEM	22
4.2.1 Initial Cost for Equipment	22
4.2.2 TSGA System Electricity Cost	24
4.2.3 Solution-Related Cost	25
4.2.4 Total Cost for TSGA System.....	27
4.3 ANALYSIS RESULTS	27
4.3.1 Results of the Scenario with a 10 Mile Distance	28
4.3.2 Sensitivity Analysis	30
4.4 DISCUSSIONS.....	35
4.4.1 Transportation Alternatives	35
4.4.2 Enhanced TSGA System.....	37
5. CONCLUSIONS AND RECOMMENDATIONS FOR FUTURE WORK.....	40
REFERENCES	42
APPENDIX A. FURTHER INFORMATION ON TSGA SYSTEM.....	A-1
APPENDIX B. FITTING CORRELATIONS OF COMPONENT PRICE	B-1
APPENDIX C. TRUCK OPERATION SCHEDULE	C-1
APPENDIX D. PIPELINE TRANSPORTATION CALCULATION.....	D-1

LIST OF FIGURES

Fig. 1. Proposed two-step looping solution for using remote low-temperature geothermal energy to cool commercial buildings.....	3
Fig. 2. Oil and natural gas production in the United States.....	4
Fig. 3. Volume of coproduced water (barrels) in 2007 by five states with the greatest generation.....	5
Fig. 4. Locations of oil and gas wells with higher than 215°F (102°C) BHT (the view was made with NREL’s Geothermal Prospector).....	6
Fig. 5. Population intensity within a 50 km radius surrounding each of the oil/gas wells in Texas that has a BHT higher than 215°F (102°C).....	7
Fig. 6. Ground temperature at 3 km below the surface in the continental United States.....	8
Fig. 7. Climate zones and associated heating and cooling degree days in the United States.....	10
Fig. 8. Dühring diagram for LiBr/H ₂ O solution with state points of the single-effect absorption process.....	11
Fig. 9. Dühring diagram for LiCl/H ₂ O solution with state points of the single-effect absorption process.....	12
Fig. 10. Dühring diagram for CaCl ₂ /H ₂ O solution with state points of the single-effect absorption process.....	13
Fig. 11. Schematic of the two-step solution looping geothermal absorption cooling.....	14
Fig. 12. A SorpSim diagram showing the simulation of the two-step absorption cooling.....	15
Fig. 13. State points of two-step geothermal absorption cooling shown on Dühring chart for LiBr-H ₂ O.....	16
Fig. 14. Flow chart for the economic viability study.....	19
Fig. 15. TSGA system initial cost breakdown.....	29
Fig. 16. TSGA system operating cost breakdown for the 10-mile scenario.....	29
Fig. 17. Levelized cost breakdown of the TSGA system of the 10-mile case.....	30
Fig. 18. Annual operating cost components vs distance.....	31
Fig. 19. Simple payback periods resulting from different building sizes and distances.....	32
Fig. 20. Simple payback against fluctuation of carrier cost.....	32
Fig. 21. Simple payback period against fluctuation of utility rate.....	33
Fig. 22. Simple payback period against solution price.....	34
Fig. 23. Levelized cost breakdown for different distances.....	34
Fig. 24. Total cost comparison between pipeline and truck for a distance of 10 miles.....	36
Fig. 25. Current TSGA operation on Dühring chart.....	37
Fig. 26. Modified TSGA operation with higher concentration on Dühring chart.....	38
Fig. 27. An example of TSGA dehumidification hybrid system.....	39

LIST OF TABLES

Table 1. Comparison between compression and absorption chillers	1
Table 2. Summary of direct use applications in the United States.....	8
Table 3. Summary of geothermal direct-use case studies	9
Table 4. Design parameters for a 900 ton (3,165 kW cooling) two-step geothermal absorption chiller	16
Table 5. Key parameters of a water-cooled centrifugal vapor compression chiller for a large office building in Houston, Texas.....	20
Table 6. Carrier cost breakdown	26
Table 7. List of variables for calculating simple payback	28
Table 8. Cost comparison between the baseline system and the TSGA system	29
Table 9. Levelized cost breakdown of the TSGA system	30
Table 10. Comparison between the costs of using pipeline and tanker trucks for transporting working fluid over a distance of 10 miles.....	35

ABBREVIATED TERMS

ASHRAE	American Society of Heating, Refrigerating and Air-Conditioning Engineers
BHT	bottom-hole temperature
COP	coefficient of performance
CPVC	chlorinated polyvinyl chloride
DOE	US Department of Energy
EFLH	equivalent full-load hour
HDPE	high-density polyethylene
HVAC	heating ventilation and air-conditioning
IC	initial cost
LCOSE	levelized cost of saved electricity
LiBr	lithium bromide
LMTD	logarithmic mean temperature difference
NREL	National Renewable Energy Laboratory
NTU	number of heat transfer units
OPC	operating cost
PCM	phase-changing material
PRH	ratio of pump flow rate to heat-rejection capacity
P-T-X	equilibrium vapor pressure, temperature, and concentration of a fluid pair
PVC	polyvinyl chloride
ROW	right of way
SMU	Southern Methodist University
TDS	total dissolved solids
TSGA	two-step geothermal absorption
UA	overall heat transfer coefficient
USGS	US Geological Survey
VC	vapor compression

EXECUTIVE SUMMARY

Low-temperature geothermal resources (less than 150°C or 300°F) are abundant in the United States. Although higher temperatures are preferred for power production, low-temperature resources can directly provide buildings with space heating or drive an absorption chiller for space cooling. Two barriers to wider utilization are the typically long distances between geothermal sources and potential end uses and the low energy density of the transported energy. An innovative two-step geothermal absorption (TSGA) system was recently proposed. With this system, the low-temperature geothermal energy is stored and transported at ambient temperature with an energy density significantly higher than that in the transportation of hot water. The higher energy density results from utilizing the high latent heat of water vaporization (970 Btu/lb) instead of the sensible heat of water (30 to 40 Btu/lb, assuming a typical 30°F to 40°F temperature change in the hot water).

A conceptual design of the TSGA system has been developed based on the conventional single-effect absorption cycle. LiBr/H₂O solution was selected as the working fluid pair because of its superior performance to other currently available fluid pairs. Key design parameters of a 900 ton two-step absorption chiller have been determined through a series of computer simulations with the SorpSim program developed at Oak Ridge National Laboratory. The computer simulation results indicate that the two-step absorption chiller has an annual average thermal coefficient of performance (COP_{th}) of 0.67. The energy density of the transported working fluid is 150 Btu_{clg}/lb (i.e., providing 150 Btu of cooling per 1 lb of transported LiBr/H₂O weak solution).

To make the TSGA system economically competitive and reliable over a long term, several technical challenges need to be addressed, including (1) minimizing the required volume and the associated transportation cost of the working fluid, (2) maintaining appropriate vacuum levels at various components of the absorption cycle, (3) retaining good quality of the working fluid during transportation and storage, and (4) harvesting heat from geothermal wells that are sparsely located and that vary in production rates.

A case study for applying the TSGA system at a large office building at Houston, Texas, indicates that, for a 10-mile distance from the geothermal site to the building, the simple payback of the TSGA system is 10.7 years compared with a conventional electric-driven vapor compression chiller. The payback of the TSGA system is highly sensitive to the distance, building size (cooling loads), transportation cost, and the electricity rate. Also, for a 10-mile distance, transporting the working fluid with tanker trucks leads to lower life cycle cost than a pipeline using high-density polyethylene pipes. The railway transportation option has a lower operating cost than the tanker truck option, but it is limited by accessibility to the railway stations.

In addition, the amount of working fluid that must be transported between the geothermal site and the building can be reduced by integrating an absorption-based dehumidifier into the proposed TSGA system in a cascade configuration. In this way, the sensible and latent cooling loads are separated and the chilled-water temperature can be elevated, which leads to an enlarged concentration difference between the strong and weak solutions and therefore an increased energy density of the transported fluid.

1. INTRODUCTION

The use of geothermal energy is an emerging area for improving the nation’s energy resiliency. Conventionally, geothermal energy applications have focused on power generation using high-temperature hydrothermal resources. However, many low-temperature (below 150°C/300°F) geothermal resources are also available but have not been utilized. For example, it is estimated that 25 billion barrels of fluid (mostly water and some dissolved solids) at 176°F to 302°F (80°C to 150°C) is coproduced annually at oil and gas wells in the United States (DOE 2015). The heat contained in coproduced geothermal fluid (usually also referred as “coproduced water”) is typically wasted because the fluid is reinjected back into the ground. In addition, there are plentiful low-temperature hydrothermal resources located throughout the United States.

Hot water from low-temperature geothermal reservoirs can be used to provide heat for industrial processes, agriculture and aquaculture, or to keep buildings warm. Such an application is usually called “direct use.” In typical direct-use applications, a well is drilled into a geothermal reservoir, and a pumping system is used to extract a steady stream of hot water from the well. The hot water then delivers heat through a heat exchanger for its intended use. The cooled water can be injected back underground or disposed of on the surface. Spent fluids from geothermal electric plants may also be subsequently used for direct-use applications in a cascaded operation (DOE 2015).

Low-temperature geothermal energy can also be used to provide space cooling and refrigeration through absorption or adsorption cooling technologies (Holdmann 2005, Lech 2009, Luo et al. 2010, Kreuter 2012, Wang et al. 2013). In 1980, a 150 ton single-stage absorption chiller was installed at the Oregon Institute of Technology to supply a base cooling load to five campus buildings, which have a total floor area of 280,000 ft². The absorption chiller used LiBr/H₂O solution and was powered with geothermal fluid at 192°F (88.9°C) (Lienau 1996). Another geothermal-powered absorption chiller in Alaska was used to produce -21°F (-29.4°C) brine to provide refrigeration for an ice museum (Holdmann 2005). Kreuter (2012) compared a conventional electric-driven vapor compression chiller with geothermal-driven absorption and adsorption chillers. The required temperature ranges of the geothermal sources and working fluids for geothermal-driven absorption and adsorption chillers are summarized in Table 1. As shown in Table 1, with adsorption technology, geothermal resources with even lower temperatures (e.g., 55°C or 131°F) can also be used to provide space cooling to buildings.

Table 1. Comparison between compression and absorption chillers (Modified based on Kreuter 2012)

Chiller type	Compression type	Energy source	Common cooling agents
Absorption	Thermal absorption loop	Heat at 185-302°F (85–150°C)	LiBr/water or water/ammonia
Adsorption	Thermal adsorption of water vapor	Heat at 131-392°F (55–200°C)	Water with solid adsorption agent (e.g., silica gel or zeolite)

Lech (2009) studied the technical and economic feasibility of a new geothermal cooling/heating system for buildings. Based on computer simulations, this study confirms that the geothermal cooling/heating system “can be operated at a generator inlet temperature of 86°C (187°F) and (condenser and absorber) cooling water temperature of 20 to 28°C (68 to 83°F). The coefficient of performance (COP), which is an indicator of the thermal efficiency of the absorption chiller, was 0.73 (for 20°C/68°F cooling water) and 0.68 (for 28°C/83°F cooling water).” It should also be noted that this COP is based on the input of thermal energy instead of the electric power, which is used in calculating the COP of electric-driven chillers. The thermal COP of an absorption chiller is thus not directly comparable with the electric COP of a conventional electric-driven chiller. The study also concludes that the single-stage geothermal hot-

water-driven absorption chiller has the least equivalent warming impact for cooling the studied building compared with a wide range of single- and double-stage absorption chillers (driven by geothermal hot water or directly fired) as well as electric-driven chillers. Wang et al. (2013) presented a techno-economical study for a conceptual design of a large-scale geothermal absorption air-conditioning system, which is proposed to provide base-load cooling to the main campus of the University of Western Australia. The study concluded that the payback period for the proposed system is around 11 to 13 years and that the economic viability of the system is “heavily reliant on the quality of the geothermal resource, drilling costs and the effects of various proposed emission trading schemes.” The European Geothermal Energy Council (EGEC 2005) projected good future development in the use of geothermal energy for cooling purposes, especially in the warmer regions of Europe. However, the report stated that “like low-temperature geothermal power production, geothermal absorption cooling is restricted to areas with geothermal resources of about 100°C (212°F) and above.”

Low-temperature geothermal resources have the potential to be used to satisfy a large portion of the heating and cooling demands in buildings. However, due to the high cost for developing pipelines over long distances, utilization of geothermal energy for space conditioning currently is limited to places where the geothermal resources are available at or very near the demand site. If the energy in low-temperature geothermal resources can be stored and transported to demand sites at a cost lower than that of pipelines, utilization can significantly increase. This can reduce greenhouse gas emissions, extend the economic life of oil and gas fields, and profitably utilize the abandoned oil and gas field infrastructure.

Two different technologies—adsorption and phase-changing material (PCM)—for transporting waste heat to provide heating over distances were compared by Storch et al. (2006). For example, for transporting the waste heat from an aluminum factory to an incineration plant 7 to 10 km (4.3 to 6.2 miles) away, the adsorption system using zeolite is more cost-effective than the PCM system. In addition, PCM system needs a longer time than the adsorption system to be charged with 446°F (230°C) hot air (5.5 hr for charging 4.1 MWh heat to the adsorption system and 9.3 hr for charging 2.4 MWh heat to the PCM system).

Jiang et al. (2015) introduced a novel system to reduce the size and the associated cost of the pipeline by transporting hot water at a larger temperature difference. The system uses two absorption heat transformers (a variation of the conventional absorption chiller): one is installed at an industrial plant, and the other is installed at the building. With the two heat transformers, the temperature difference between the supply and return of the pipeline can be increased to 117°F (65°C), which is about two to three times higher than the conventional systems, which directly circulate hot water between the industry plant and the building. The larger temperature difference allows a lesser amount of water to be circulated while providing the same amount of heat, which means smaller pipes and lower cost for the pipeline. It was reported that the added capital cost of the heat transformers would be less than the reduced cost of the pipeline and the associated pumping power if the transportation distance were more than 20 km (12.4 miles).

ORNL proposed the development of a two-step geothermal absorption (TSGA) system that uses low-temperature geothermal energy to provide space conditioning for buildings located more than 10 miles away from geothermal resources. Figure 1 is a schematic of the proposed technology, which decouples the production and regeneration of the conventional absorption cycle into a two-step process. The first step is regeneration and takes place near the geothermal resource. A weak aqueous solution of lithium bromide (LiBr) or another salt solution is heated using geothermal heat to drive off moisture from the solution. The concentrated solution is then allowed to cool to ambient temperature at the geothermal site and is transported to commercial or industrial buildings by tanker trucks (or other appropriate means,

including, but not limited to, trains or ships).¹ The second step is space conditioning at the building site, where liquid water is evaporated to provide cooling and the water vapor is absorbed at low pressure by the concentrated solution, which is kept near ambient temperature. The diluted solution is then transported back to the geothermal site to regenerate (concentrate) it.

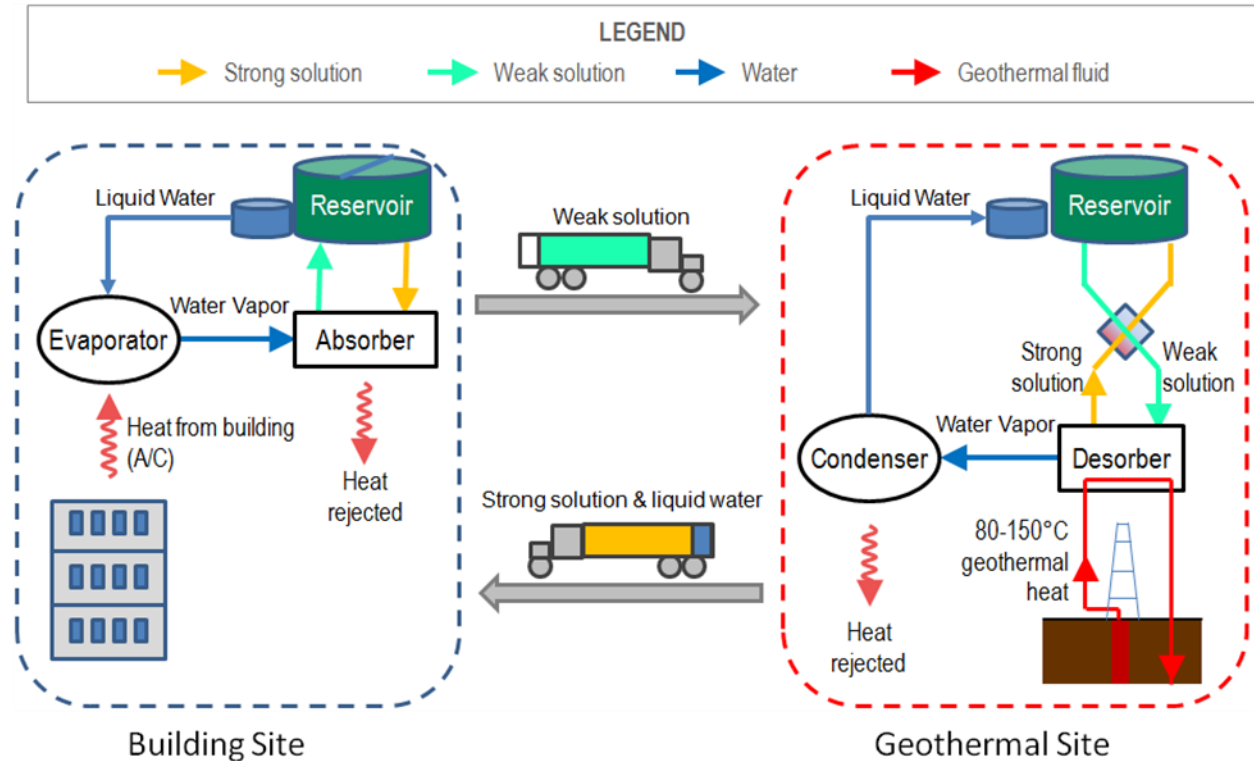


Fig. 1. Proposed two-step looping solution for using remote low-temperature geothermal energy to cool commercial buildings.

This study assesses the technical challenges and the economic viability of the TSGA system. A case study is conducted to evaluate the cost-effectiveness of the TSGA system compared with a conventional electric-driven vapor compression chiller and the impacts of various parameters on the economic viability of the TSGA system.

¹ LiBr solution is not hazardous as defined by 49 CFR 172.101 by the U.S. Department of Transportation. Shipments of LiBr solution require no hazardous shipping labels. Shipments by post, parcel, air, water, rail, or truck are acceptable within each carrier's weight limits and packaging requirements (<http://www.seiberlich.com/files/msds/LIB00006.pdf>).

of the nearly 1 million actively producing oil and gas wells in the United States in 2007. The five states with the greatest coproduced water volumes were Texas, California, Wyoming, Oklahoma, and Kansas. The coproduced water volumes from these states represent nearly 75% of total US production (onshore and offshore) as shown in Fig. 3. With more than 216,000 active oil and gas wells statewide, Texas alone contributed 7.4 billion bbl of coproduced water, which accounts for 35% of the total volume of coproduced water generated in the United States. On average, an oil/gas well in Texas produced 93.6 bbl of water each day. More than 75% of oil wells in the United States are classified as “stripper” wells. On average, each of these stripper wells produces about 2 bbl of oil per day. The water-to-oil ratio of stripper wells can be as high as 40 bbl of water to 1 bbl of oil produced (API 2006). It indicates that the coproduced water is widely dispersed.

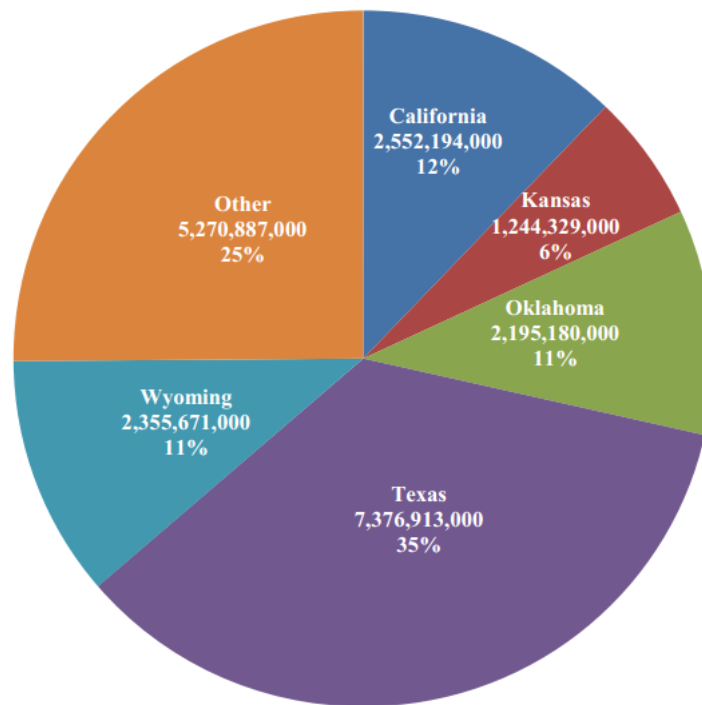


Fig. 3. Volume of coproduced water (barrels) in 2007 by five states with the greatest generation. (Source: Clark and Veil 2009)

The quality of coproduced water varies across the United States. National-level data for the chemistry of coproduced water are available from the US Geological Survey (USGS) Produced Water Database (USGS 2015), and state-specific data are usually collected by and stored in databases of oil- and gas-producing states. Many water chemistry databases only provide values of total dissolved solids (TDS), but others include detailed cation and anion concentrations. Coproduced water with a TDS less than 10,000 mg/L may be used for industrial and agricultural activities, while water with a TDS greater than 50,000 mg/L will likely require injection disposal for proper management (IOGCCAC 2006). Depending on the quality of the coproduced water, appropriate heat exchangers and maintenance procedures shall be used to extract heat from the coproduced water.

National Renewable Energy Laboratory (NREL) developed a web-based geographic information system application, Geothermal Prospector,⁴ to support resource assessment and data exploration for geothermal energy. The oil and gas well data collected by Southern Methodist University’s (SMU’s) Geothermal

⁴ http://maps.nrel.gov/gt_prospector

Laboratory are accessible through Geothermal Prospector. Figure 4 shows the locations of oil and gas wells with a BHT higher than 215°F (102°C). However, data for the coproduced water flow rate at each oil/gas well are not accessible from Geothermal Prospector. As can be seen in Fig. 4, most oil and gas wells in the United States that have a BHT higher than 215°F (102°C) are located in the South and the West, while there are some wells with high BHT in Pennsylvania and West Virginia.

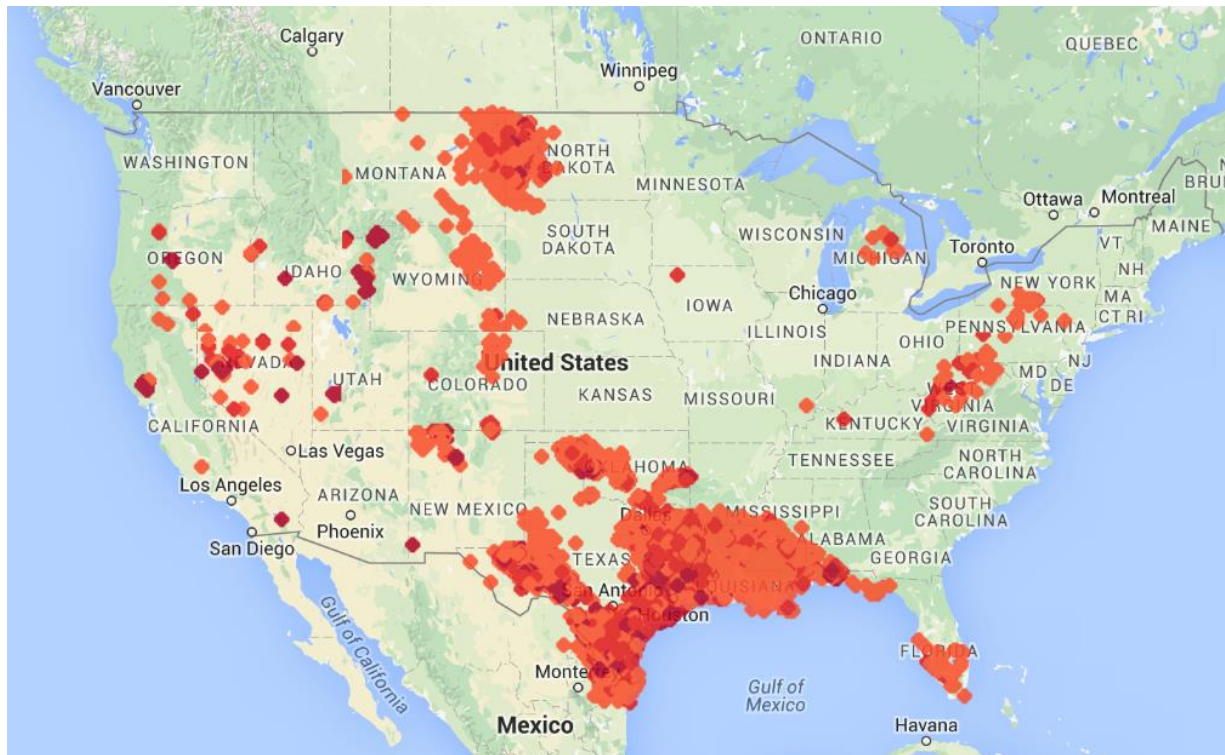


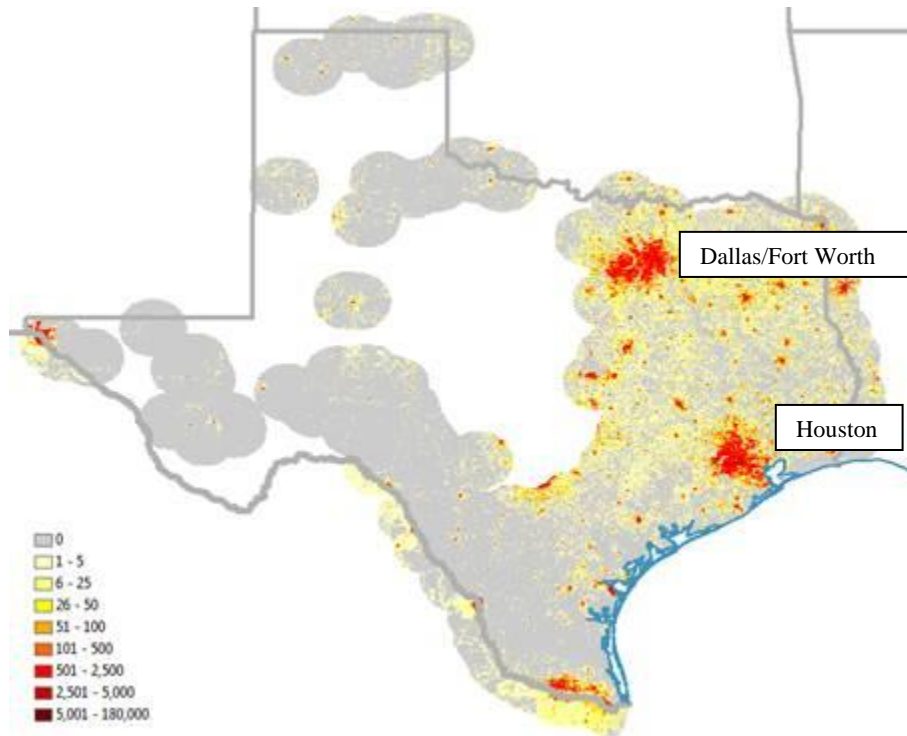
Fig. 4. Locations of oil and gas wells with higher than 215°F (102°C) BHT (the view was made with NREL’s Geothermal Prospector).

Figure 5 illustrates the population density within a 50 km radius surrounding each of the oil/gas wells in Texas that have a BHT higher than 215°F (102°C). The population data are from ORNL’s LandScan™ dataset and are the finest resolution (at approximately 1 km resolution) global population distribution data available.⁵ As shown in Fig. 5, except for the wells in or around the Dallas/Fort Worth and Houston areas, most wells are located in areas that have a population density of less than 50 people/km² (indicated by yellow color) within the 50 km radius surrounding the well. This indicates that there may not be enough demand within a short distance of these wells for use of this energy to be cost-effective.

In addition to distance, there are other challenges associated with using coproduced water: (1) fouling and corrosion of the heat exchanger (depending on the site-specific chemistry of the coproduced water), which will increase the operating and maintenance cost of the system and reduce the economic benefits; (2) dispersed nature of the resource; and (3) the reliability of the coproduced water. The quantities of coproduced water from oil and gas wells are highly variable from field to field (Nordquist 2009). Furthermore, the dynamics of coproduced water quantities can also vary as the field is developed. While conventional fields typically yield more water as production progresses, nonconventional fields, such as

⁵ <http://web.ornl.gov/sci/landscan/>

coal bed natural gas, shale and diatomite, and dewatering,⁶ might yield less water as production progresses (IOGCCAC 2006).



Different color indicates different population density (i.e., population within approximately 1 km² area)

Fig. 5. Population intensity within a 50 km radius surrounding each of the oil/gas wells in Texas that has a BHT higher than 215°F (102°C).

2.2 GEOTHERMAL DIRECT USE

Most of the shallow or near-surface low-temperature geothermal resources are located in the western part of the country. A survey of 10 western states identified more than 9,000 thermal wells and springs, more than 900 low-temperature geothermal resource areas, and hundreds of direct-use sites (DOE 2015). However, low-temperature geothermal resources are also available in other areas at deeper depths. Figure 6 shows a map of the ground temperature at a 3 km (9,842 ft) depth below the surface for the continental United States, which was originally developed by the Geothermal Laboratory at SMU.⁷ Figure 6 indicates that the ground temperature at a 9,842 ft (3 km) depth below the surface is higher than 212°F (100°C) in most parts of the western states, but it is within 167–212°F (75–100°C) in most other parts of the United States and higher than 212°F (100°C) in some areas in Texas, Louisiana, Arkansas, Oklahoma, Nebraska, and Mississippi.

⁶ These nonconventional fields use a large volume of water to facilitate the production of natural gas and oil.

⁷ <http://www.smu.edu/Dedman/Academics/Programs/GeothermalLab/DataMaps/TemperatureMaps>

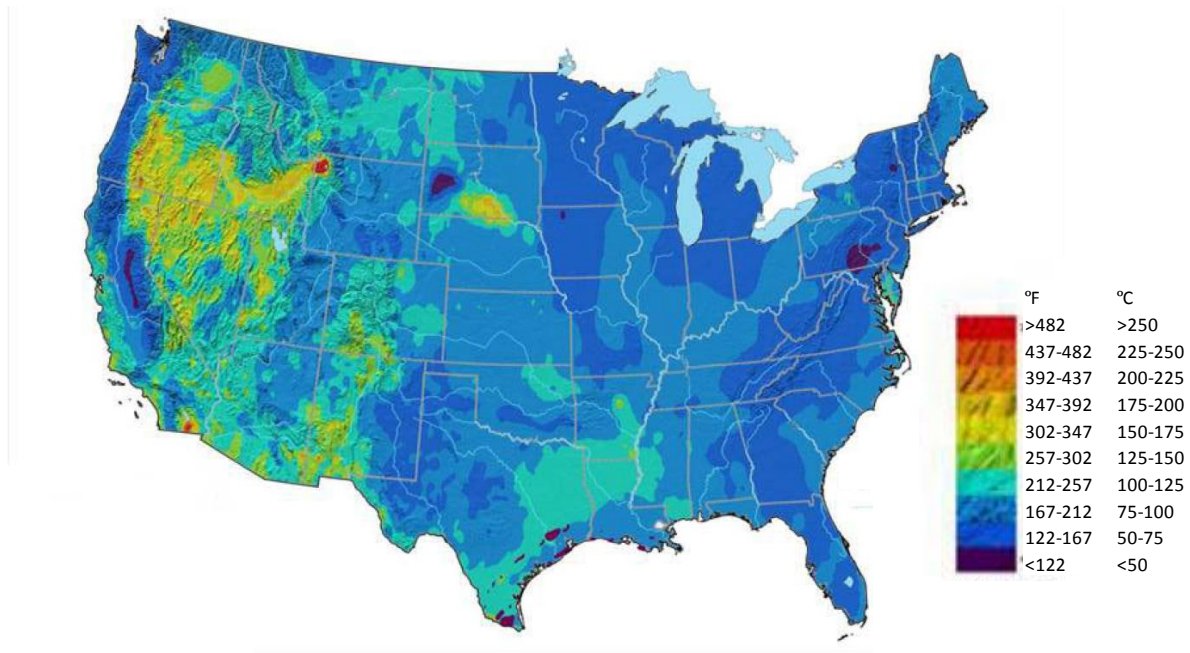


Fig. 6. Ground temperature at 3 km below the surface in the continental United States.
(Source: IOGCCAC 2006)

It is predicted that resources with temperatures less than 90°C (194°F) in the United States have the potential to provide 42,600 MW_{th} of beneficial heat (Williams 2013). Hot water extracted from low-temperature geothermal reservoirs can be used to provide heat for industrial processes and agricultural/aquaculture production or to keep buildings warm. Table 2 summarizes the direct-use applications in the United State (Boyd 2015, Lund 2015). As can be seen from Table 2, the primary uses of the low-temperature geothermal energy is to heat buildings, either through a district heating system or using one well per building.

Table 2. Summary of direct use applications in the United States

Application	Number	Peak thermal load (MW)	Annual thermal load (TJ)
District heating	19+	81.6	839.6
Space heating	2,000+	139.9	1,360.6
Industrial and agricultural drying	7	37.8	493.1
Greenhouse	45	96.9	799.8
Aquaculture	51	142	3,074
Resorts and spas	242	122.9	2,557.5
Snow melting	6	2.5	20

Direct use of low-temperature geothermal energy for space heating and/or water heating is much less expensive than using traditional fuels if the geothermal resources are near the buildings. It is reported that geothermal district heating systems can save consumers 30% to 50% in heating costs compared with natural gas heating (DOE 2015).

In a report of geothermal direct-use case studies (GHC 2005), 14 direct-use applications in the United States and Canada were presented. The locations, application types, geothermal resource information, and annual heating energy provided by these direct-use applications are summarized in Table 3. The capital and operating costs of the direct-use systems depend greatly on accessibility and chemical properties of the extracted hot water from the low-temperature geothermal resources. In all of these case studies, the geothermal resource is either at the demand site or within a distance of 2 miles. The chemical properties of the hot water determine not only the materials used for the heat exchangers and the pipelines but also the disposal cost of the hot water after extracting heat from it. If the chemical content of the spent water is not deemed as proper to dispose of on the surface by local environmental regulations, additional wells will have to be drilled and operated to inject the spent water back underground.

Table 3. Summary of geothermal direct-use case studies

Location	Type	Resource-load distance	Geothermal resource	Temperature (°F)	Annual load (MMBTU)
California Correctional Center, Susanville CA	Space heating, greenhouse	2 miles	Two 1,400 ft deep wells	165–169	52,500
Ouray hot springs pool, Ouray CO	Hot spring resort	1 mile	Spring water 1 mile from site and artesian well on site without pumps	124–145	48,000
“Gone fishing” project, Klamath falls OR	Aquaculture	On site	Six wells	80–200	4,380
Fairmont hot springs resort, Fairmont MT	Hot spring resort	On site	Spring water and a well	143–175	43,800
Philip SD	District heating	On site	Single 4,266 ft artesian well	175	3,900
Milgro greenhouse, Newcastle UT	Greenhouse	On site	Two wells	205	93,000
Kah-nee-ta swimming pool, Warm Springs OR	Hot spring resort	On site	Warm springs nearby	128	30,000
Residential downhole heat exchanger, Klamath Fall OR	Space heating	On site	One 200 ft well, no pumps, cycle driven by thermal syphoning	140	164
Oregon Trail Mushrooms, Vale OR	Cooling	On site	One 250 ft well, driving a 400 ton LiBr absorption chiller	220	Replace 43,000 MMBTU of natural gas demand

The low-temperature geothermal resources used for direct use typically contain lower levels of gas and dissolved solids than the higher-temperature fluids used for power generation (DOE 2004). Most direct-use geothermal wells are drilled using conventional water-well technology and equipment, which have less impact than the drilling technologies used for geothermal power plants or oil/gas wells.

3. TWO-STEP GEOTHERMAL ABSORPTION COOLING SYSTEM

3.1 TARGET BUILDINGS

Energy use for space conditioning in buildings depends on many factors, including the local weather, use of the building, and size of the building. As shown in Fig. 7, the US territory can be divided into five climate zones based on heating and cooling degree days, which are usually used to indicate the demands for space cooling and space heating. The southeastern part of the United States has the highest cooling degree days, which means the greatest demand for space cooling in buildings.

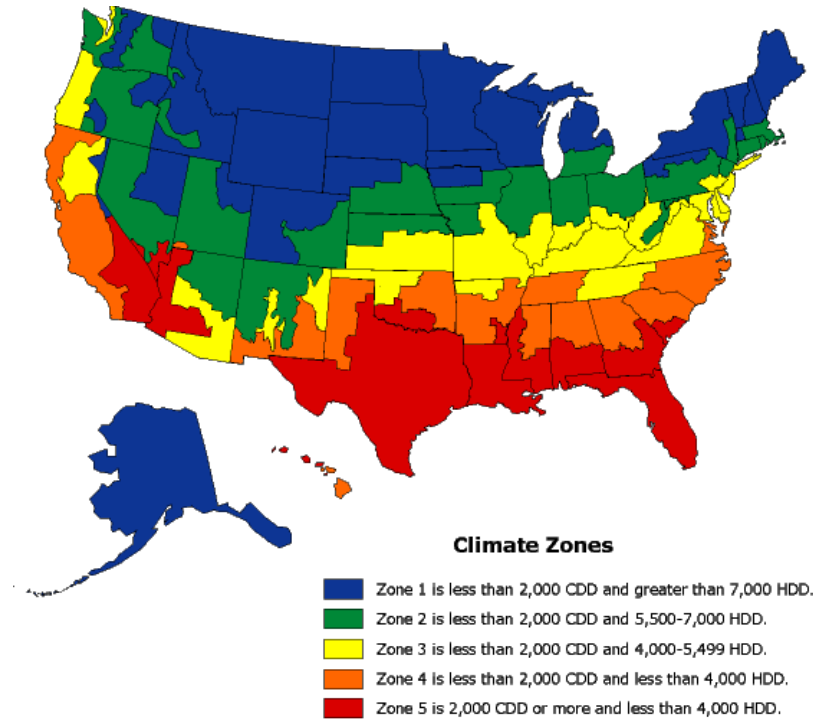


Fig. 7. Climate zones and associated heating and cooling degree days in the United States. (Source: <http://buildingsdatabook.eren.doe.gov/CBECS.aspx>).

The ideal candidate buildings for a TSGA system shall have large peak and cumulative cooling loads to take advantage of economies of scale (i.e., reducing the initial cost) and to have sufficient energy savings to offset cost premiums of the TSGA system compared to conventional space conditioning systems. Given the geographical distribution of the climate zones and the available geothermal resources, especially the free coproduced water, the target buildings for applying the TSGA system are thought to be large commercial buildings, such as schools, hospitals, and office complexes, located in the South and the West of the United States (e.g., Texas).

According to the 2009 *Buildings Energy Data Book* (BEDB) (DOE 2009), space heating and space cooling were responsible for 12.6% and 12.1%, respectively, of the 17.9 quadrillion Btu total primary energy consumption in the commercial building sector in 2006. With regard to energy expenditure, \$22.3 billion and \$19.3 billion were spent in 2006 on providing space heating and space cooling for the US commercial buildings, respectively. Natural gas is the predominant energy source on a site energy basis (68% of site energy) for space heating, while electricity is the predominant energy source (97% of site

energy) for space cooling. Space cooling and space heating in US commercial buildings resulted in 130.3 and 127.4 million metric tons of the carbon emissions in 2006.

3.2 SELECTION OF WORKING FLUID PAIR

Various fluid pairs (a pair is a refrigerant and an absorbent) can be used for absorption cooling, including LiBr/H₂O, LiCl/H₂O, CaCl₂/H₂O, H₂O/NH₃, LiNO₃/NH₃, and NaSCN/NH₃. The refrigerant in these fluid pairs is either H₂O or NH₃. Due to various regulations for transportation, application, and storage, NH₃-based fluid pairs were not considered for the TSGA system.

Selection of fluid pair for the TSGA system affects the amount of working fluid required to satisfy the cooling load, which determines the working fluid related initial costs and the operating cost associated with transporting the working fluid. The required amount of working fluid shall be minimized to reduce the initial and operating cost of the TSGA system.

Relevant properties of three H₂O-based fluid pairs were evaluated in this study. One of the most important factors considered is the equilibrium vapor pressure properties (often referred to as P-T-X data, referring to the interrelationship of equilibrium vapor pressure, temperature, and concentration of the fluid pair). The P-T-X properties determine the concentrations of strong and weak solutions, which in turn determine the energy density of the transported working fluid. Figures 8 through 10 are the Dühring diagrams for LiBr/H₂O, LiCl/H₂O, and CaCl₂/H₂O solutions, respectively, with state points of the conventional single-effect absorption process shown on them. As shown in these figures, at 45°F (7°C) chilled-water temperature and 104°F (40°C) saturated water vapor (dew point) temperature, LiBr/H₂O fluid pair works with a larger difference in the concentration of the absorbent between the strong and weak solutions than the other two fluid pairs, which leads to a lesser amount of working fluid needed for providing the same amount of cooling. For example, 17% more working fluid would have been needed if LiCl/H₂O were used instead of the LiBr/H₂O. Therefore, LiBr/H₂O is selected as the fluid pair for the TSGA system.

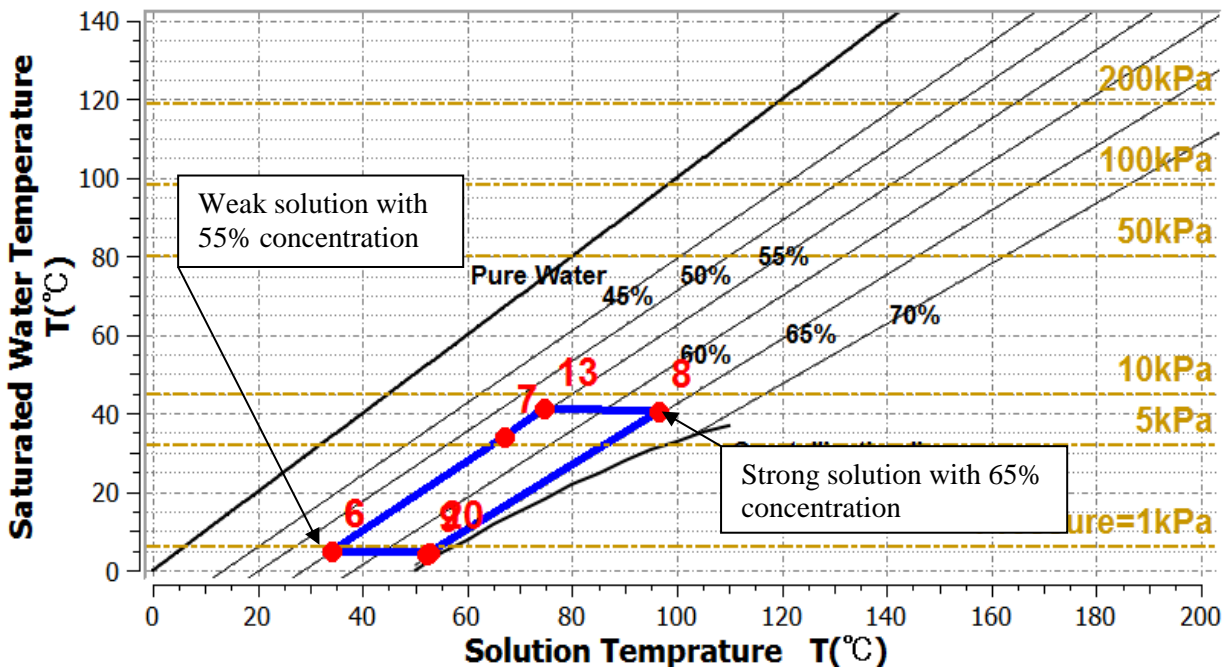


Fig. 8. Dühring diagram for LiBr/H₂O solution with state points of the single-effect absorption process. (Generated with ORNL's SorpSim Program)

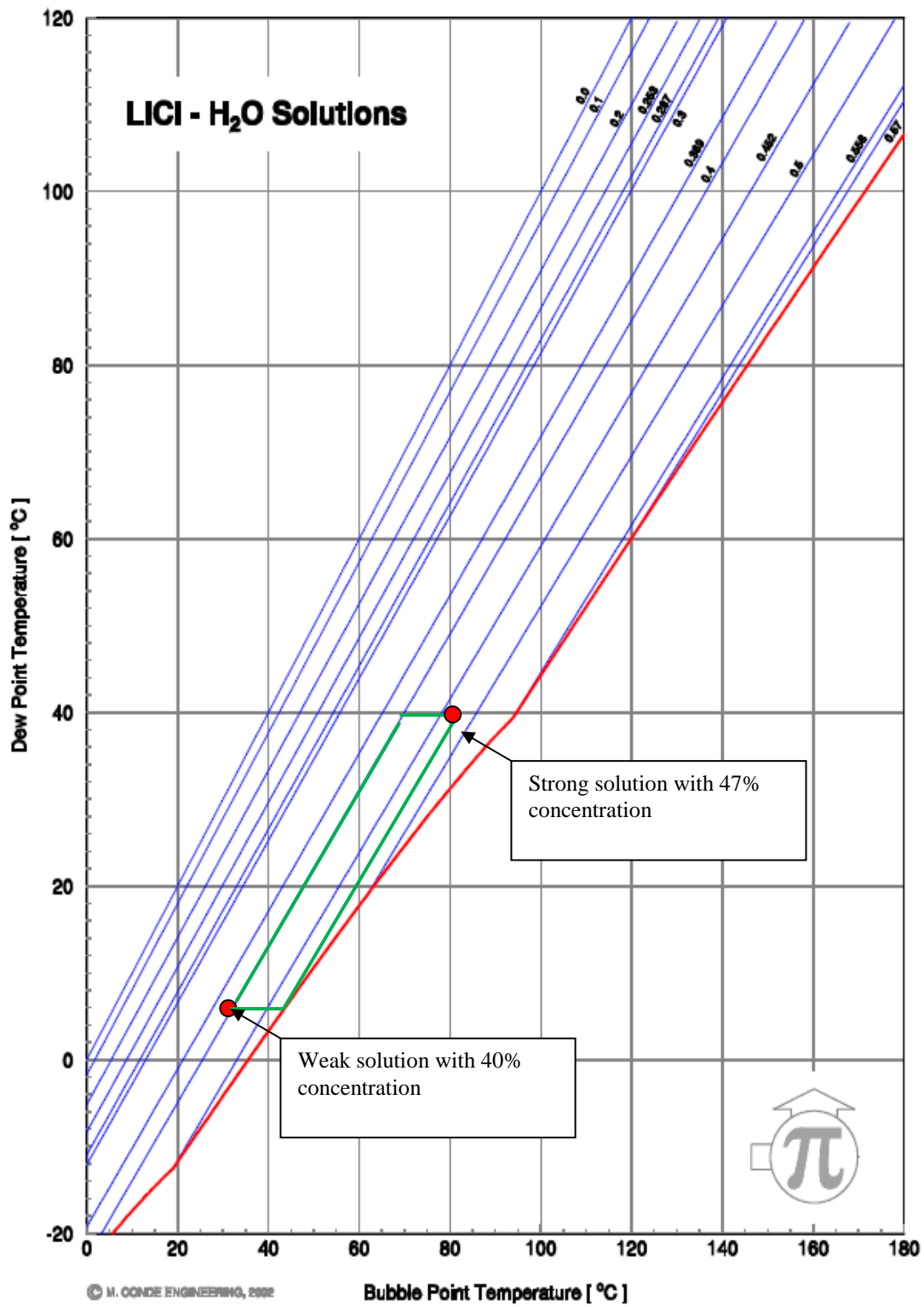


Fig. 9. Dühring diagram for LiCl/H₂O solution with state points of the single-effect absorption process. (Based on the thermal property map generated by Conde-Petrit et al. 2014)

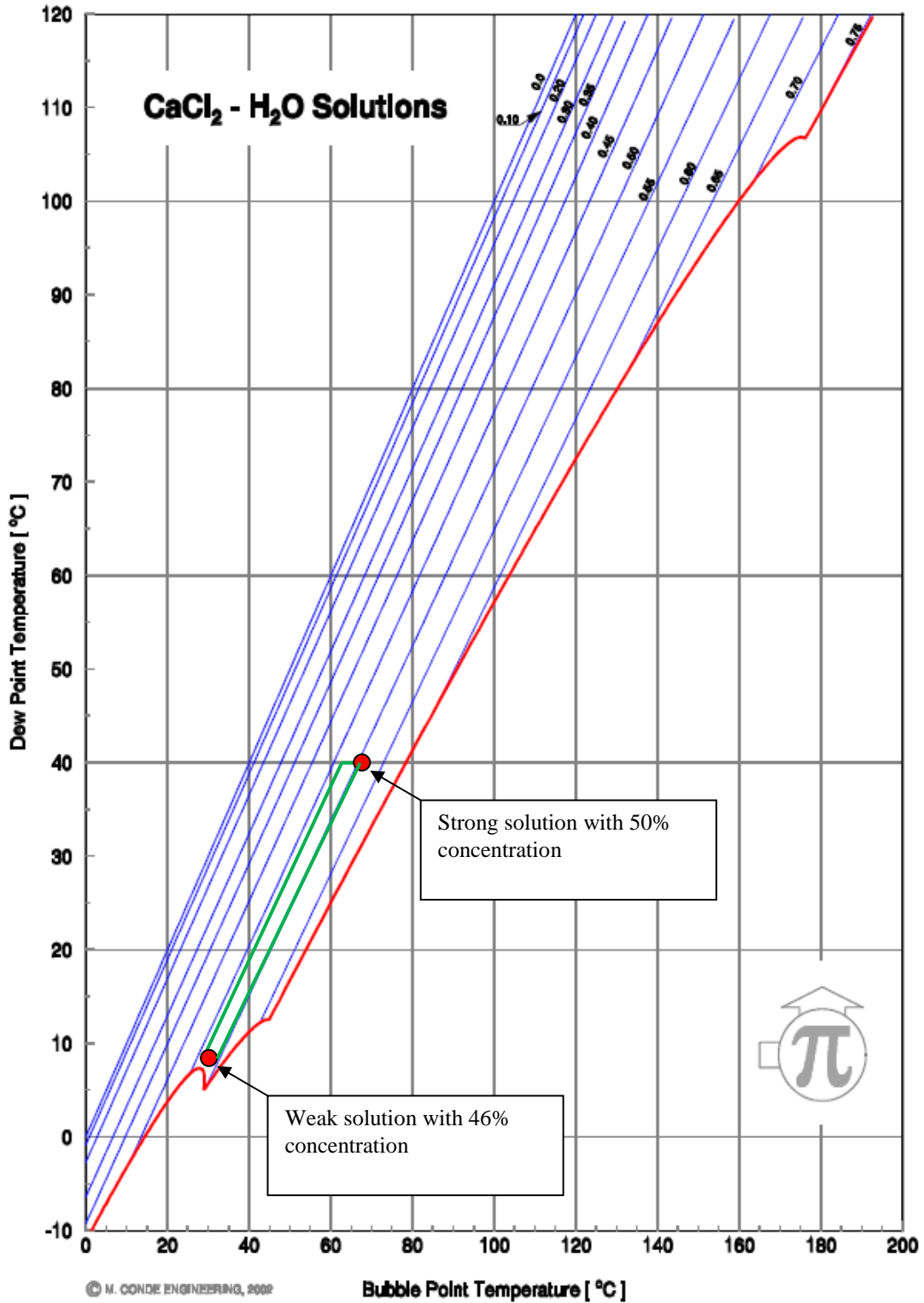


Fig. 10. Dühring diagram for CaCl₂/H₂O solution with state points of the single-effect absorption process. (Based on the thermal property map generated by Conde-Petrit et al. 2014)

3.3 DESIGN SPECIFICATION OF A 900 TON TWO-STEP GEOTHERMAL ABSORPTION CHILLER

The proposed TGSA system utilizes a split single-effect absorption cycle, which is more cost-effective than other absorption cycles for utilizing the low-temperature geothermal energy, as suggested in a previous study (Lech 2009). Figure 11 shows the diagram of a proposed TGSA system.

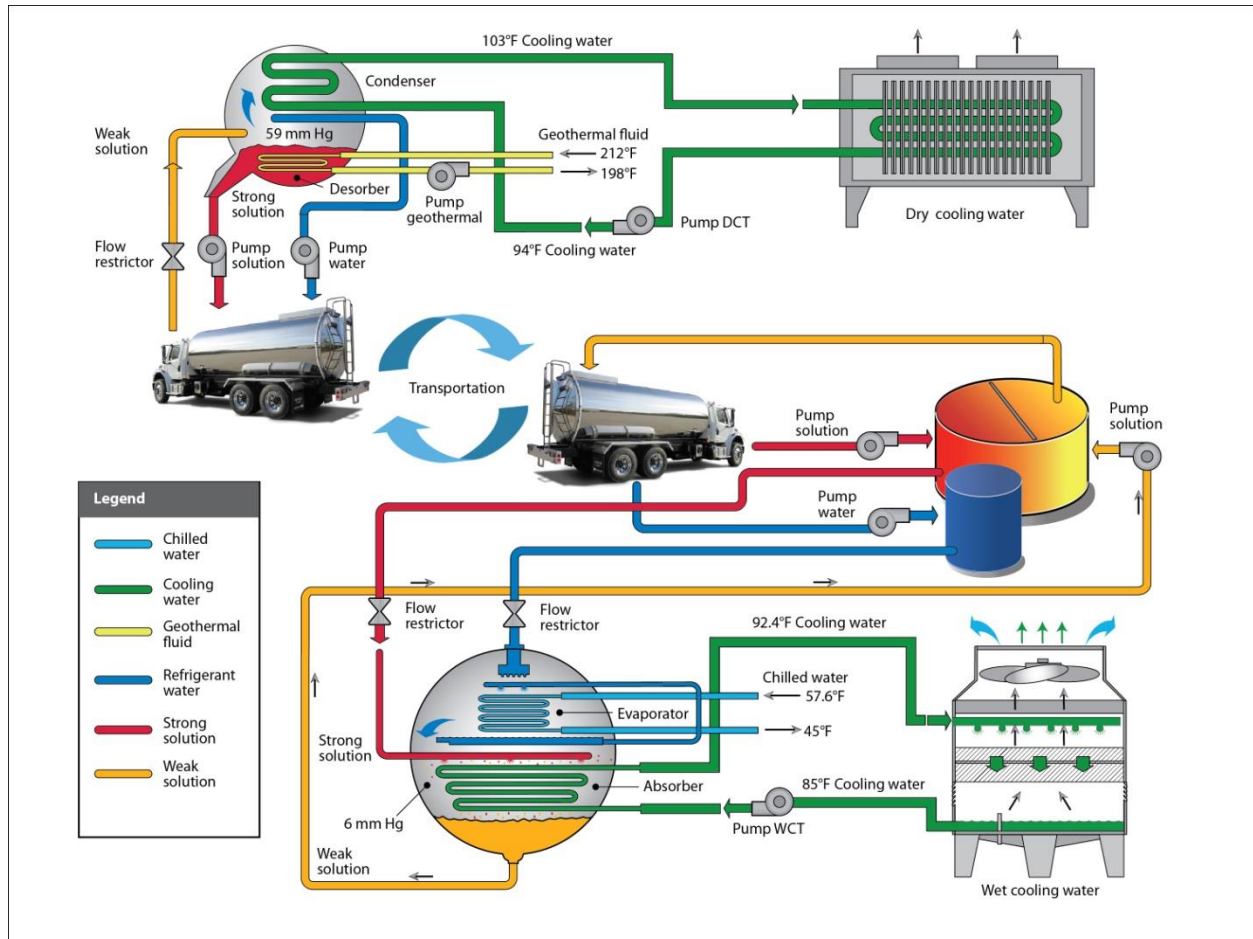


Fig. 11. Schematic of the two-step solution looping geothermal absorption cooling.

The equipment at the geothermal site includes an assembly of desorber and condenser, a cooling tower, and a circulation pump associated with the cooling tower. The function and design considerations for each of these components are discussed in Appendix A.

The equipment at the building site includes an assembly of absorber and evaporator, two flow restrictors, a wet cooling tower and an associated circulation pump, holding tanks, and a solution pump. The function and design considerations for each of these components are discussed in Appendix A.

To evaluate the economic viability of the proposed TSGA cooling system, major components of the TSGA system are sized for the targeted building and the available low-temperature geothermal resource. The design parameters for each major component are determined based on simulation results using ORNL's SorpSim program. SorpSim, a modular computer program for simulation of absorption systems, is developed based on the original ABSIM program (Grossman 1998). From the thermodynamic point of view, the two-step absorption cooling is basically a single-effect absorption cycle operated with heat from

the low-temperature geothermal resources. A computer simulation of the two-step absorption cooling is created with SorpSim; a diagram of the simulation is shown in Fig. 12. In this simulation, LiBr/H₂O solution is used as the working fluid. A dry cooler is used for the condenser at the geothermal site, and a wet cooling tower is used for the absorber at the building site.

The absorption system at the building site was sized to handle the peak cooling load of the building. The key design conditions are listed below:

- Total cooling capacity is 900 tons (3,165 kW cooling)
- Chilled water supply temperature is 45°F (7.2°C)
- Fluid supply temperature to desorber (from geothermal resource) is 212°F (100°C)
- Fluid supply temperature to condenser (from the dry cooler) is 94°F (34.4°C)
- Fluid supply temperature to absorber (from the wet cooling tower) is 85°F (29.4°C)

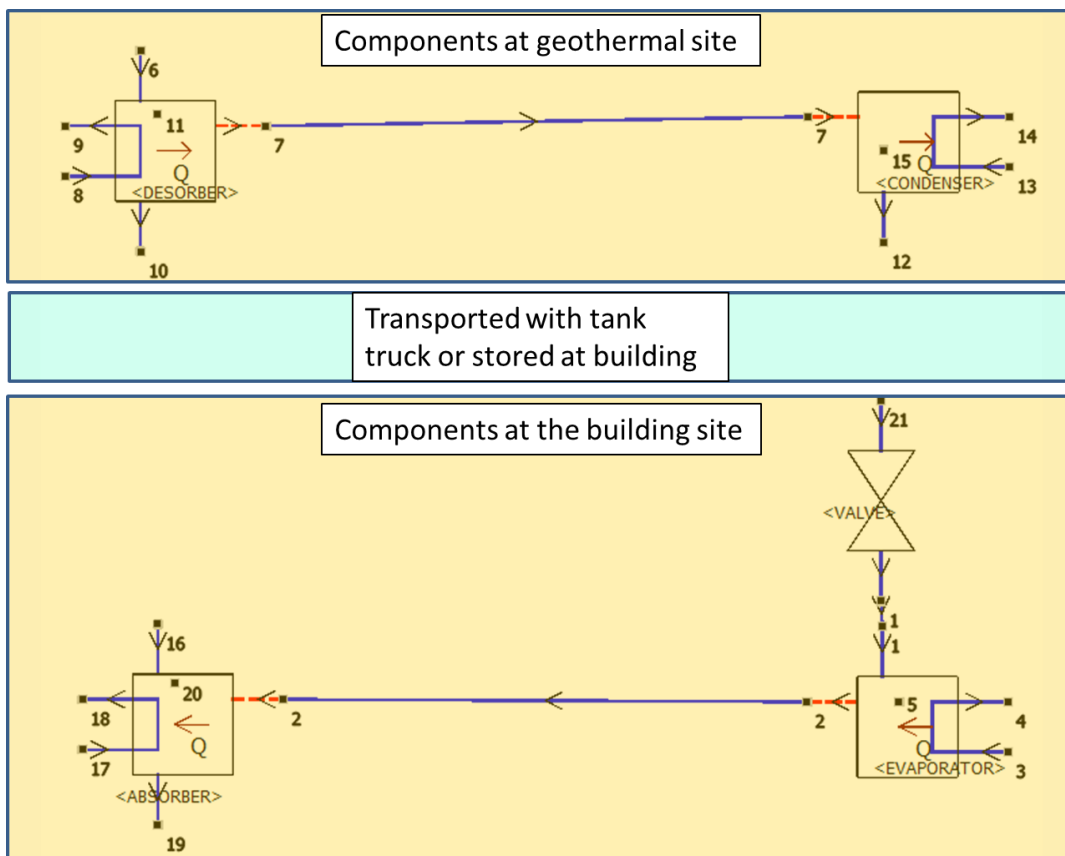


Fig. 12. A SorpSim diagram showing the simulation of the two-step absorption cooling.

The simulation-predicted thermodynamic process of the two-step geothermal absorption cooling is overlaid on the Dühring chart for the LiBr/H₂O solution in Fig. 13. The line from state point #11 to #10 indicates the desorbing process, where the water vapor pressure in the absorber is maintained at 7.8 kPa (by the condenser) and the LiBr/H₂O solution is concentrated from 53.1% to 61.9% by the heat from the geothermal resource. The line from state point #20 to #19 indicates the absorbing process, where the water vapor pressure in the absorber is maintained at 0.83 kPa (by the absorber) and the LiBr/H₂O solution is diluted from 62% to 53% by absorbing the water vapor. Table 4 lists the design parameters of the major components.

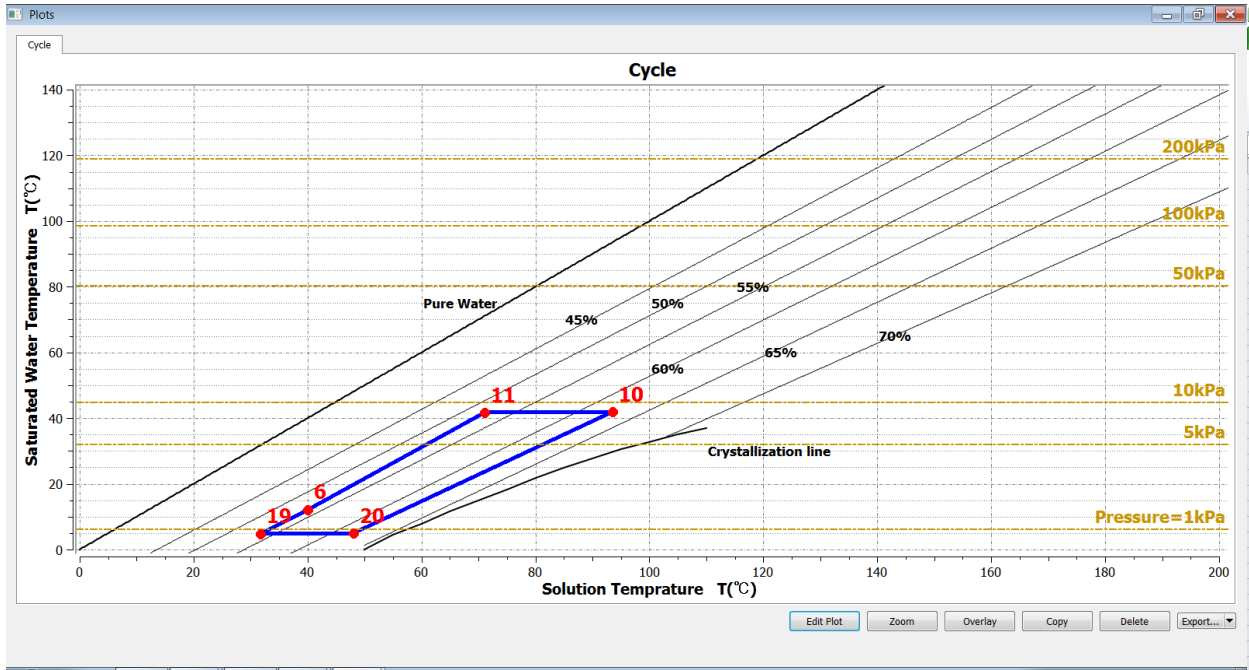


Fig. 13. State points of two-step geothermal absorption cooling shown on Dühring chart for LiBr-H₂O.

Table 4. Design parameters for a 900 ton (3,165 kW cooling) two-step geothermal absorption chiller

Type	UA value (kW/°C)	NTU (-)	Effectiveness (-)	Closest approach (°C)	LMTD (°C)	Heat load (kW)
Evaporator	600	1.2	0.712	2.844	5.644	3388
Desorber	350	1.6	0.73	8.272	14.38	5032
Condenser	1000	1.5	0.776	1.533	3.55	3551
Absorber	700	2.9	0.912	1.522	5.411	3789

The size and design parameters for the accessory equipment are listed below:

- Cooling tower (at building site)
 - Type: Wet
 - Design supply temperature: 85°F (29.4°C)
 - Flow rate: 3,487 GPM (220 kg/s)
 - Cooling capacity at design condition: 1,082 tons (3,789 kW)
- Cooling tower (at geothermal site)
 - Type: Dry
 - Design supply temperature: 94°F (34.4°C)
 - Flow rate: 2,536 GPM (160 kg/s)
 - Cooling capacity at design condition: 933 tons (3,551 kW)
- Pumps
 - For dry cooling tower (Pump_{DCT}): 2,536 GPM (160 kg/s) flow, 30 ft (9.2 m) head
 - For wet cooling tower (Pump_{WCT}): 3,487 GPM (220 kg/s) flow, 30 ft (9.2 m) head
 - For geothermal fluid (Pump_{geothermal}): 2,409 GPM (168 kg/s) flow, 30 ft (9.2 m) head
 - For solution (Pump_{Solution}): 198 GPM (12.5 kg/s) flow, 40 ft (12.2 m) head

- For refrigerant water (PumpWater): 19.8 GPM (1.25 kg/s) flow, 40 ft (12.2 m) head
- Tanker truck: 5,000 gal (18.75 m³), insulated, pressurized with inert gas. This tanker truck load is determined based the maximum allowed gross vehicle weight of 80,000 lb and the empty vehicle weight for the Class 8B truck, which is about 20,000 lb according to US National Research Council (2010).
- Trailer tanks: three 5,000 gallon (18.75 m³), insulated, pressurized with inert gas.

Based on the simulation results, the thermal efficiency, COP_{th} , and solution energy density of the TSGA chiller is calculated with Eq. (1) and (2), respectively:

$$COP_{th} = \frac{\text{Cooling output at evaporator}}{\text{Heat input at the desorber}} \quad (1)$$

$$\text{Solution Energy Density} = \frac{\text{Cooling output}}{\text{Mass of weak solution}} \quad (2)$$

The calculated COP_{th} is 0.67 and the solution energy density is 150 Btu/lb (349 kJ cooling energy for each kilogram of weak solution).

3.4 TECHNICAL CHALLENGES FOR TWO-STEP ABSORPTION

In contrast to conventional absorption chillers, which recirculate a small amount of working fluid in a closed-loop cycle, the proposed two-step absorption system has an open-loop absorption process—a strong solution from a holding tank goes into the absorber and becomes a weak solution, and then the weak solution is discharged to another holding tank. To reduce the frequency and associated costs of transportation, a large amount of working fluid needs to be stored in the holding tanks and the tanker truck. These unique characteristics bring in a few significant technical challenges, which are discussed below along with possible solutions.

3.4.1 Increase Energy Density of Transported Material/Minimize Amount of Working Fluid

The required amount of working fluid (e.g., LiBr/H₂O) affects not only the initial cost of the system (including the cost for the working fluid and the holding tanks to store it) but also the operating cost of the system (including the cost for transporting the working fluid with a tanker truck and pumping the solution between the low-pressure assemblies and the holding tanks or trucks). These costs can all be reduced by improving the solution energy density by maximizing the difference in the concentration of the absorbent between the strong and weak solutions. One solution is to integrate an absorption dehumidifier into the TSGA system, which is discussed later in Section 4.4.2.

3.4.2 Prevent Air Infiltration

For transported energy solutions that utilize a working fluid with sub-atmospheric pressure (as in a LiBr/H₂O-based TSGA), the risk for air ingress could be higher than in a conventional closed-cycle absorption chiller. The absorption of water vapor is highly dependent upon an internal vacuum being maintained. Loss of vacuum from an air leak will cause reduced system capacity. In addition, as air leaks into any component, it introduces oxygen, which in turn accelerates corrosion. It is thus important to minimize air leaks in all the components of the TSGA system. To prevent air from infiltrating the holding tanks and the tanker, these containers can be very slightly pressurized relative to ambient with oxygen-free gas (e.g., Nitrogen). The low-pressure assemblies in the geothermal and building sites shall also

equipped with a purging system for air and any other gases (for example, products of corrosion such as H_2).

3.4.3 Maintain Quality of Working Fluid

Given the need for a large amount of working fluid, and the risk of exposure to air, it is critical to maintain working fluid of good quality for a long time period (10–20 years). In the presence of dissolved oxygen, a LiBr/ H_2O solution is aggressive to many metals, including carbon steel and copper. Following design considerations and routine maintenance are needed to maintain the quality of working fluid, including (1) periodically adding a corrosion inhibitor, (2) periodically adding a pH buffer, and (3) including appropriate filters in the working-fluid pipeline.

4. ECONOMIC ANALYSIS

This chapter presents a case study of utilizing the TSGA system to replace a conventional electric-driven vapor compression chiller for space cooling. The purpose of this case study is twofold: (1) to evaluate the economic viability of the TSGA system and (2) to investigate the impacts of various parameters on the economic viability of the TSGA system.

To evaluate the economic viability of the TSGA system, its initial and operating costs are compared with a baseline system (a conventional water-cooled electric-driven vapor compression chiller). The compared cost components and the evaluation procedure are shown in Fig. 14.

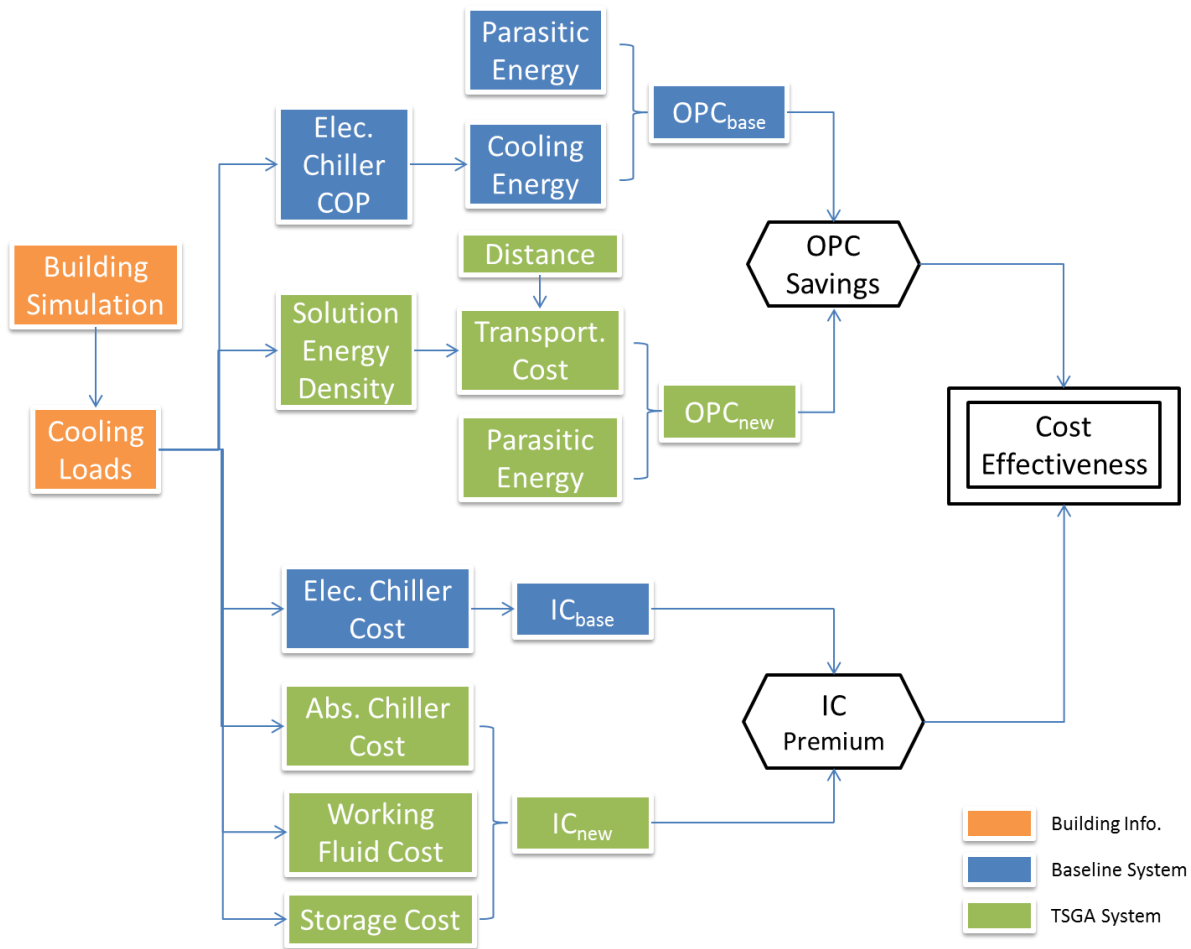


Fig. 14. Flow chart for the economic viability study.

The operating cost of the baseline system (OPC_{base}) is the electricity cost for operating the chiller and the associated equipment (i.e., cooling tower and circulation pump), which is determined by the cooling demand and the chiller efficiency. The operating cost of the TSGA system (OPC_{new}) includes the parasitic electricity cost (for operating the cooling tower and circulation pumps) and the cost for transporting working fluid (e.g., LiBr/H₂O solution) back and forth between the geothermal site and the building. The initial cost of the baseline system (IC_{base}) includes the costs for the electric-driven vapor compression chiller and associated equipment, but the initial cost of the TSGA system (IC_{new}) includes the cost of the working fluid and storage tanks in addition to the cost of the absorption chiller and the associated

equipment. With the cost difference in the initial cost and the operating cost of the two systems, the cost-effectiveness of the TSGA system can be evaluated with different performance metrics (e.g., simple payback and the levelized cost of saved electricity). Algorithms for calculating the initial cost and operating cost of the two systems are introduced in following sections.

A case study for applying the TSGA system in a large office building in Houston, Texas, is conducted. A computer model of a large office building adopted from the DOE Commercial Reference Building Models⁸ is used in this case study. The modeled building has a total floor space of 498,588 ft² (46,320m²), and it is designed in accordance with the American Society of Heating Refrigerating and Air-Conditioning Engineers (ASHRAE) Standard 90.1-2004 (ASHRAE 2004). Details of this building are described in a technical report (Deru et al. 2011). The initial cost premium and the operating cost savings of the TSGA system are calculated; then the simple payback and the levelized cost of saved electricity are evaluated. Furthermore, a series of sensitivity analyses are carried out to illustrate the impacts of various parameters on the cost-effectiveness of the TSGA system. In addition, transportation costs of three different means (i.e., tanker truck, pipeline, and railway) are compared, and the possible approaches to improve the cost-effectiveness of the TSGA system are discussed.

4.1 BASELINE COOLING SYSTEM

The baseline cooling system for the large office building includes two water-cooled electric-driven centrifugal vapor compression (VC) chillers with a total capacity of 871 tons (3063 kW_{clg}), a wet cooling tower, a pump to circulate condensing water between the cooling tower and the chiller, and other HVAC components inside the building, such as the distribution system for the chilled water, air-handling-unit, fan coils, or other heat-transfer terminals. The nominal efficiency (electrical coefficient of performance or COP_{el}) of the chillers is 5.5. Table 5 lists the key parameters of the VC chiller used in this case study.

Table 5. Key parameters of a water-cooled centrifugal vapor compression chiller for a large office building in Houston, Texas

Parameter	TSGA case study value
Chiller capacity	871 ton (3063 kW _{clg})
Annual chiller energy consumption	2,219 MWh
Equivalent full load hour	2209 h/year
Annual operational COP _{el} of chiller	3.05
Annual cooling load	6,767,238 kWh _{clg} /year

Simulation with the building model predicts that the chiller consumes 2,219 MWh of electricity each year. The annual operational COP_{el} (COP_{el,avg}) of the chiller is determined with the equivalent full-load hours (EFLH) of typical office buildings in the Houston area, the predicted chiller power consumption ($Energy_{chiller}$), and the chiller capacity ($Capacity_{chiller}$), as expressed by Eq. (3):

$$COP_{el,avg} = \frac{EFLH * Capacity_{chiller}}{Energy_{chiller}} \quad (3)$$

According to a report published by ASHRAE, the EFLH of a typical office building in the Houston, Texas, area is 2,209 h/year (Carlson 2001).

⁸ The model and the simulation results are available at: http://energy.gov/sites/prod/files/2013/12/f5/refbldg_largeoffice_new2004_v1.3_5.0.zip

The annual cooling load of the building can be calculated with Eq. (4):

$$Cooling\ load = Energy_{chiller} * COP_{el,avg} \quad (4)$$

4.1.1 Initial Cost

The initial cost of the baseline system is the sum of the installed cost of its components, which depends on the size of each component. For a given size of the chiller, the size of the other components can be determined. Cooling tower capacity (Q_{vcCT}) is determined using the energy balance of the VC cycle as expressed in Eq. (5):

$$Q_{vcCT} = P_{vcchiller} + Q_{vcchiller} = \left(1 + \frac{1}{COP_{design-vc}}\right) * Q_{vcchiller} \quad (5)$$

where $P_{vcchiller}$, $Q_{vcchiller}$, and $COP_{design-vc}$ are the power input, capacity, and nominal efficiency of the VC chiller, respectively. With the above calculated cooling tower size, the condensing water loop circulation pump flow rate (M_{vcpump}) is determined using the ratio of the pump flow rate to the heat rejection capacity (PRH), of which the rule-of-the-thumb value is 3gpm/ton, as shown in Eq. (6):

$$M_{vcpump} = PRH * Q_{vcCT} \quad (6)$$

The installed costs of the chiller ($Cost_{vcchiller}$), cooling tower ($Cost_{vcCT}$), and pump ($Cost_{vcpump}$) are estimated using *RSMeans Mechanical Cost Data* (Reed Construction 2010), which includes costs of material, labor, and overhead and profit to purchase and install these equipment. A series of cost-size correlations were generated for the chiller, cooling tower, and pump, as shown in Eqs. (7), (8), and (9), respectively, using the cost data over a range of sizes listed in the RSMeans database. These correlations are then used to predict the installed cost of each equipment with given capacity:

$$Cost_{vcchiller} = A_{vcchiller} * Q_{vcchiller} + B_{vcchiller} \quad (7)$$

$$Cost_{vcCT} = A_{CT} * Q_{vcCT} + B_{CT} \quad (8)$$

$$Cost_{vcpump} = A_{pump} * M_{vcpump} + B_{pump} \quad (9)$$

In above equations, A and B with different subscripts are correlation coefficients, which are derived from the RSMeans data for different equipment. These coefficients are listed in Appendix A.

The initial cost of the baseline system (IC_{vc}) can be expressed by inserting Eqs. (7), (8), and (9) into Eq. (10).

$$IC_{vc} = Cost_{vcchiller} + Cost_{vcCT} + Cost_{vcpump} \quad (10)$$

4.1.2 Operating Cost

Because the operation of the cooling tower and the condensing water pump is usually synchronized with chiller's operation, their electricity consumptions can be predicted based on the chiller's energy consumption ($Energy_{vcchiller}$). The pump energy consumption ($Energy_{vcpump}$) is approximated as a fraction of $Energy_{vcchiller}$ as expressed with Eq. (11), where RP is the ratio of pumping energy to the chiller energy.

$$Energy_{vc_{pump}} = Energy_{vc_{chiller}} * RP \quad (11)$$

Similarly, the annual energy consumption of the cooling tower ($Energy_{CT}$) is approximated with $Energy_{vc_{chiller}}$ and a ratio RCT as expressed by Eq. (12):

$$Energy_{vc_{CT}} = Energy_{vc_{chiller}} * RCT \quad (12)$$

The consumption of electrical energy by the baseline system (Ele_{vc}), which does not include the components inside the building, is the sum of the electricity consumed by the VC chiller, the condensing water pump, and the cooling tower, as expressed by Eq. (13):

$$Ele_{vc} = Energy_{vc_{chiller}} + Energy_{vc_{pump}} + Energy_{vc_{CT}} = Energy_{vc_{chiller}} * (1 + RP + RCT) \quad (13)$$

Values of RP and RCT are obtained from the computer simulation of the baseline system. The operating cost of the baseline system (OPC_{vc}) is the product of the local electricity rate (UR) and Ele_{vc} as expressed in Eq. (14).

$$OPC_{vc} = UR * Ele_{vc} \quad (14)$$

4.2 TSGA SYSTEM

The TSGA system consists of a two-step absorption chiller, a dry cooler at the geothermal site, a wet cooling tower at the building, two pumps to circulate condensing water at both sites, and two storage tanks at the building site. Tanker trucks are selected in this case study as the means of transportation for the working fluid. Calculations for the initial and operating costs of the TSGA system are described in the following sections.

4.2.1 Initial Cost for Equipment

The two-step absorption chiller of the TSGA system has the same cooling capacity as the VC chiller of the baseline system. Based on this chiller capacity, the sizes of the cooling tower and the circulation pump used in the TSGA system are calculated.

The heat input at desorber (Q_{des}) can be calculated from the capacity (Q_{evap}), which is equal to $Q_{vc_{chiller}}$, and COP_{th} of the two-step absorption chiller, as expressed in Eq. (15):

$$Q_{des} = \frac{Q_{evap}}{COP_{th}} \quad (15)$$

The Q_{des} calculated in Eq. (15) is the required capacity of the desorber (i.e., the maximum heat transfer rate between the geothermal fluid and the desorber). In this study, the quality of the geothermal fluid (i.e., coproduced water) is assumed to be good enough so that it can directly exchange heat with the desorber without an intermediate heat exchanger. At occasions where the water chemistry imposes a threat of corrosion, an intermediate heat exchanger might be needed to isolate the geothermal fluid from the desorber while allowing heat transfer.

As introduced in Chapter 3, there are two heat rejection components in the TSGA system: a dry cooler for the condenser at the geothermal site and a wet cooling tower for the absorber at the building site. To simplify the analysis in this study, the two cooling towers are assumed to have same capacities. The total

required capacity of these two cooling towers (Q_{absCT}) can be calculated using energy balance of the absorption cycle as expressed in Eq. (16):

$$Q_{absCT} = Q_{des} + Q_{evap} = \left(1 + \frac{1}{COP_{th}}\right) * Q_{evap} \quad (16)$$

With the calculated cooling tower capacity, the combined flow rate ($M_{abs_{pump}}$) of the two condensing water pumps can be determined using *PRH*, as shown in Eq. (17):

$$M_{abs_{pump}} = PRH * Q_{absCT} \quad (17)$$

In addition to the two condensing water pumps, the TSGA system needs another pump at the geothermal site to circulate the hot geothermal fluid through the heat exchanger in the desorber. According to the SorpSim simulation described in Chapter 3, the design flow rate of this pump is about 40% of the flow rate of the combined condensing water pumps. Additional pumps to draw the working fluid from the desorber and absorber and the condensed water from the condenser into the storage tank and the tanker truck (as shown in Fig. 11) are needed as well. The cost of these pumps is denoted as $Cost_{extpump}$, and is estimated as a fraction of the installed cost of the condensing water pump in the baseline system ($Cost_{vc_{pump}}$).

The installed costs of the absorption chiller ($Cost_{abs_{chiller}}$), cooling tower ($Cost_{absCT}$), and pump ($Cost_{abs_{pump}}$) are estimated using *RSMeans Mechanical Cost Data* (Reed Construction 2010). It is assumed that the two-step absorption chiller uses the same components as the conventional packaged absorption chiller and thus has the same price as the conventional absorption chiller.

A series of cost-size correlations were generated for the absorption chiller, cooling tower, and pump, as shown in Eqs. (18), (19), and (20), respectively, using the equipment cost data over a range of sizes. These correlations are then used to predict the installed costs of each equipment for a given capacity within the range available in the RSMeans database:

$$Cost_{abs_{chiller}} = A_{abs_{chiller}} * Q_{evap} + B_{abs_{chiller}} \quad (18)$$

$$Cost_{absCT} = 2 * \left[A_{CT} * \frac{1}{2} * \left(1 + \frac{1}{COP_{th}}\right) * Q_{evap} + B_{CT} \right] \quad (19)$$

$$Cost_{abs_{pump}} = 2 * (1 + 40%) * \left[A_{pump} * PRH * \frac{1}{2} * \left(1 + \frac{1}{COP_{th}}\right) * Q_{evap} + B_{pump} \right] + Cost_{extpump} \quad (20)$$

In above equations, A and B with different subscripts are correlation coefficients derived from the RSMeans data for different equipment. These coefficients are listed in Appendix A.

The initial cost of the main equipment of the TSGA system ($Cost_{abs_{eqp}}$) is calculated with Eq. (21):

$$Cost_{abs_{eqp}} = Cost_{abs_{chiller}} + Cost_{absCT} + Cost_{abs_{pump}} \quad (21)$$

4.2.2 TSGA System Electricity Cost

The components of the TSGA system that consume electricity are the cooling towers and the circulation pumps. The electricity consumed by these components can be estimated based on the electricity consumption of their counterparts in the baseline system.

Assuming that the cooling tower of the TSGA system has the same efficiency as the cooling tower used in the baseline system and that its electricity consumption ($Energy_{absCT}$) is linearly related to the amount of the condensing heat dissipated by the cooling tower (Eq. 22), $Energy_{absCT}$ can then be calculated based on the baseline cooling tower energy consumption and the ratio of the condensing heat between the baseline system and the TSGA system, as expressed in Eq. (23).

$$\frac{Energy_{absCT}}{Energy_{vcCT}} = \frac{Q_{absCT}}{Q_{vcCT}} \quad (22)$$

$$Energy_{absCT} = RCT * Energy_{vcchiller} * \frac{1 + \frac{1}{COP_{th}}}{1 + \frac{1}{COP_{design-vc}}} \quad (23)$$

Assuming the condensing pump of the TSGA system has the same efficiency and head as the condensing pump used in the baseline system, the ratio of the condensing pump energy consumptions between the two systems is the same as the ratio of the heat rejection loads of the two systems. In addition, because the geothermal fluid pump operates with the same head but with 40% flow rate of the two condensing pumps combined, its electricity consumption is 40% of that consumed by the two condensing pumps. The solution pumps also consume electricity but at a much smaller rate due to their much lower flow rate compared with the other pumps. The total electricity consumption of the solution pumps, denoted as $Energy_{extpump}$, is estimated as a fraction of energy use of the condensing pumps in the baseline system. Thus Eq. (24) can be used to calculate the total pumping energy consumption:

$$Energy_{abspumps} = RP * Energy_{vcchiller} * \left[(1 + 0.4) * \frac{1 + \frac{1}{COP_{th}}}{1 + \frac{1}{COP_{design-vc}}} \right] + Energy_{extpump} \quad (24)$$

The total electricity consumption of the TSGA system (Ele_{abs}) is calculated with Eq. (25):

$$\begin{aligned} Ele_{abs} &= Energy_{abspumps} + Energy_{absCT} \\ &= \left[(1.4 * RP + RCT) * \frac{1 + \frac{1}{COP_{th}}}{1 + \frac{1}{COP_{design-vc}}} \right] * Energy_{vcchiller} + Energy_{extpump} \end{aligned} \quad (25)$$

The electricity cost of the TSGA system ($Cost_{absELE}$) is calculated with Eq. (26):

$$Cost_{absELE} = UR * Ele_{abs} \quad (26)$$

4.2.3 Solution-Related Cost

Two types of costs are associated with the working fluid used in the TSGA system: (1) the initial cost of purchasing a sufficient amount of working fluid to ensure continuous operation of the two-step absorption chiller and (2) the cost of transporting the working fluid between the geothermal site and the building.

4.2.3.1 Solution energy density

The minimum amount of working fluid and the frequency of transportation needed to satisfy a given cooling demand depend on the energy density of the working fluid ($Energy_{den}$), which is the amount of cooling energy delivered with a unit mass of working fluid. The cooling provided by the absorption chiller is a result of the water vapor evaporation at the evaporator. The amount of evaporated water (M_w) can be computed based on the concentration of the absorbent (i.e., LiBr) in the strong and weak solutions (C_{SS} and C_{WS} , respectively) and the mass of the weak solution (M_{WS}), as expressed in Eq. (27):

$$M_w = \frac{C_{SS} - C_{WS}}{C_{SS}} M_{WS} \quad (27)$$

The provided cooling (Q_{cool}) is the product of the calculated M_w and evaporation heat of water (h_{fg}). The solution energy density, which is evaluated based on the mass of the weak solution of the working fluid, can then be calculated with Eq. (28):

$$Energy_{den} = \frac{Q_{cool}}{M_{WS}} = \frac{M_w * h_{fg}}{M_{WS}} = \frac{(C_{SS} - C_{WS}) * h_{fg}}{C_{SS}} \quad (28)$$

4.2.3.2 Cost of transportation

The tanker truck operation is scheduled to ensure continuous operation of the TSGA system as described in Appendix C. The annual total operating time of the tanker truck (T_{total}) can be calculated for a given distance between the geothermal site and the building (D), annual equivalent full load hour ($EFLH$), velocity of the truck (V), trailer switching time (T_{switch}), cooling energy at peak hour ($Q_{clgpeak}$), solution energy density ($Energy_{den}$), and the capacity of the tanker truck (M_{TL}). Equation (29) expresses the calculation:

$$T_{total} = \frac{EFLH * 2 * \left(\frac{D}{V} + T_{switch} \right) * Q_{clgpeak}}{Energy_{den} * M_{TL}} \quad (29)$$

The annual cost of transportation ($Cost_{abstrans}$) is the product of the average carrier cost (TR) and T_{total} as expressed in Eq. (30):

$$Cost_{abstrans} = TR * T_{total} \quad (30)$$

Table 6 lists the breakdown of the national average of carrier cost in 2012 (Fender and Pierce 2013), which is based on an average transportation speed of 40 mph. For the 10-mile distance used in this case study and considering the time for switching trailer tanks at the geothermal and building sites, the truck will travel only 24 miles instead of 40 miles in each hour. Thus the costs for fuel, repair and maintenance, and tires are adjusted based on the actual travel distance (as highlighted in Table 6) while keeping other costs intact. The adjusted total carrier cost per hour is \$52.2/h.

Table 6. Breakdown of average carrier cost for 2012

Item	Average cost per hour (\$)	
	Original	Adjusted ^a
Fuel	25.63	15.44
Truck lease or purchase payments	6.94	6.94
Repair and maintenance	5.52	3.32
Truck insurance premiums	2.51	2.51
Permits and licenses	0.88	0.88
Tires	1.76	1.06
Tolls	0.74	0.74
Driver wages	16.67	16.67
Driver benefits	4.64	4.64
Total	65.29	52.20

^a The adjustments to the costs for fuel, repair and maintenance, and tires are based on the actual distance traveled.

In addition to the tanker truck, three trailer tankers are needed to keep the absorption chiller operating continuously: two at the building site and one at the geothermal site. The cost of trailer tankers ($Cost_{abs_{tank}}$) is calculated with Eq. (31) using a typical price of trailer tankers ($Price_{tank}$), which is \$35,000 per trailer tanker.

$$Cost_{abs_{tank}} = 3 * Price_{tank} \quad (31)$$

4.2.3.3 Solution initial cost

For each tanker truck used for transporting solution between geothermal site and the building, a truckload of working fluid needs to be purchased. The total number of the tanker trucks is determined from the annual total operating time calculated in Eq. (29) and the annual EFLH, as expressed in Eq. (32). The truck operation is explained in Appendix C.

$$N_{truck} \geq \frac{T_{total}}{EFLH} = \frac{2 * \left(\frac{V}{V} + T_{switch}\right) * Q_{clg_{peak}}}{Energy_{int} * M_{TL}} \quad (32)$$

The amount of solution to purchase is related to the total number of trucks and trailer tankers in the system. Since one of the trailer tanks at the building site is always empty at the beginning of an operation cycle, the total amount of solution ($N_{solution}$) is expressed in Eq. (33):

$$N_{solution} = N_{truck} + 2 = \frac{2 * \left(\frac{V}{V} + T_{switch}\right) * Q_{clg_{peak}}}{Energy_{int} * M_{TL}} + 2 \quad (33)$$

The cost of purchasing solution ($Cost_{absolution}$) is expressed in Eq. (34):

$$Cost_{abs_{solution}} = Price_{solution} * M_{TL} * \left(\frac{2 * \left(\frac{V}{V} + T_{switch} \right) * Q_{clg_{peak}}}{Energy_{int} * M_{TL}} + 2 \right) \quad (34)$$

4.2.4 Total Cost for TSGA System

The total initial cost of the TSGA system (IC_{abs}) is the sum of the equipment cost, the solution cost, and the cost of the three trailer tanks, as shown in Eq. (35):

$$IC_{abs} = Cost_{abs_{eqp}} + Cost_{abs_{solution}} + Cost_{abs_{tank}} \quad (35)$$

The total operating cost for the TSGA system (OPC_{abs}) is the sum of its electricity cost and transportation cost, as shown in Eq. (36):

$$OPC_{abs} = Cost_{abs_{ele}} + Cost_{abs_{trans}} \quad (36)$$

4.3 ANALYSIS RESULTS

The cost-effectiveness of the TSGA system is evaluated with two metrics: (1) simple payback period and (2) levelized cost of saved electricity (LCOSE). The simple payback period is the time period that the capital cost premium is recovered with the cumulative operating cost savings achieved by the TSGA system. The LCOSE indicates the cost for saving each kilowatt hour of the electric energy by replacing the baseline system with the TSGA system over a given time period.

The simple payback period (SP) is calculated using Eq. (37):

$$SP = \frac{IC_{abs} - IC_{vc}}{OPC_{vc} - OPC_{abs}} \quad (37)$$

The capital costs and annual operating costs of both systems are calculated using the equations described in Sections 4.1 and 4.2. By assembling all the related equations into Eq. (37), the simple payback period can be expressed by Eq. (38):

$$SP = \frac{\left[P_{ac} - P_{vc} + P_{CT} \times \left(\frac{1}{COP_{th}} - \frac{1}{COP_{design-vc}} \right) + P_{pump} \times PRH \times \left(\frac{1.4}{COP_{abs}} - \frac{1}{COP_{design-vc}} \right) \right] \times CS + Cost_{extpump} + P_{solution} \times M_{TL} \times (N + 2) + 3 \times P_{tanker}}{UR \times \left\{ CP \times \left[1 + \left(1 - 1.4 \times \frac{1 + \frac{1}{COP_{th}}}{1 + \frac{1}{COP_{design-vc}}} \right) \times RP + \left(1 - \frac{1 + \frac{1}{COP_{th}}}{1 + \frac{1}{COP_{design-vc}}} \right) \times RCT \right] - Energy_{extpump} \right\} - TR \times EFLH \times N} \quad (38)$$

where, N represents the ratio of the total cooling demand at peak load condition during the round trip of a truck to the maximum cooling energy delivered by a truckload of solution, as expressed in Eq. (39):

$$N = \frac{2 * \left(\frac{V}{V} + T_{switch} \right) * Q_{clg_{peak}}}{Energy_{den} * M_{TL}} \quad (39)$$

Other previously not defined variables in Eq. (38) are explained in Table 7.

The LCOSE is calculated using Eq. (40):

$$LCOSE = \frac{Investment}{Electricity\ Saved} = \frac{(IC_{abs} - IC_{vc}) + \sum_{k=1}^n [OPC_{abs} / (1 + DR)^k]}{\sum_{k=1}^n [(Ele_{vc} - Ele_{abs}) / (1 + DR)^k]} \quad (40)$$

As expressed in Eq. (40), LCOSE is the ratio of all the investment needed to save electricity, which includes the initial cost premium and the cumulative operating cost over a given time period (e.g., the lifespan of the system), to the cumulative electricity savings over the same time period. In this study, a 20-year lifespan [the value of n in Eq. (40)] and a 3% discount rate (DR) are assumed when calculating LCOSE.

In this section, the economical effectiveness of the TSGA system is evaluated for a scenario in which the distance between the geothermal site and the building is 10 miles. Results of a series of sensitivity studies are then presented to discuss the sensitivity of the economical effectiveness to various parameters.

Table 7. List of variables for calculating simple payback

Notation	Description	Unit
P_{ac}	Normalized cost of absorption chiller	\$/ton
P_{vc}	Normalized cost of vapor compression chiller	\$/ton
P_{CT}	Normalized cost of cooling tower	\$/ton
P_{pump}	Normalized cost of pump	\$/gpm
CS	Chiller Size	ton
CP	Annual power consumption of vapor compression chiller	kWh/year

4.3.1 Results of the Scenario with a 10 Mile Distance

The size and initial cost of major equipment used in the TSGA and the baseline systems, as well as the annual operating cost of the two systems, are calculated using the procedures and equations described in Sections 4.1 and 4.2 and listed in Table 8. The ratio between the pump flow rate and cooling tower capacity is set as $PRH = 3$ gpm/ton. The pump and cooling tower energy consumption ratios (to the baseline chiller energy consumption) are $RP = 5\%$ and $RCT = 9\%$, which is predicted by the benchmark model for the large office building. The initial cost and energy consumption of the small pumps for solution and refrigerant water ($Cost_{extpump}$, $Energy_{extpump}$) in the TSGA system are estimated as 50% of that of the condensing pump used in the baseline system.

Figure 15 shows the initial capital cost breakdown of the TSGA system. The top three contributors to the initial cost are the absorption chiller, solution, and the cooling tower, which together contribute 89.1% of the total initial cost of the TSGA system.

The operating cost of the TSGA system is categorized into (1) the electricity cost for running the cooling towers and pumps and (2) the transportation cost of renting and operating the tanker trucks. As shown in Fig. 16, in the 10-mile distance scenario, the transportation cost represents over half of the total operating cost.

Based on the initial costs and the annual operating costs of the two systems, the simple payback of the TSGA system for the 10-mile distance scenario is 10.7 years.

Table 8. Cost comparison between the baseline system and the TSGA system

Cost type	Item	Baseline system	TSGA system
Initial cost (\$)	Chiller	420,578	660,131
	Pumps	11,161	37,436
	Cooling tower	103,861	212,737
	Solution	-	289,845
	Trailer tanks	-	105,000
	Total initial cost		535,601
Operating cost (\$)	Electricity	255,519	71,887
	Transportation	-	111,669
	Total operating cost	255,519	183,556

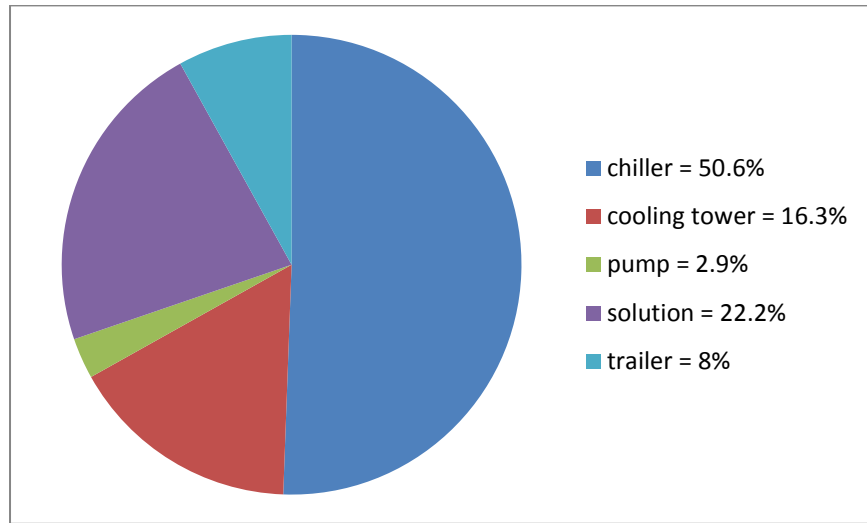


Fig. 15. TSGA system initial capital cost breakdown.

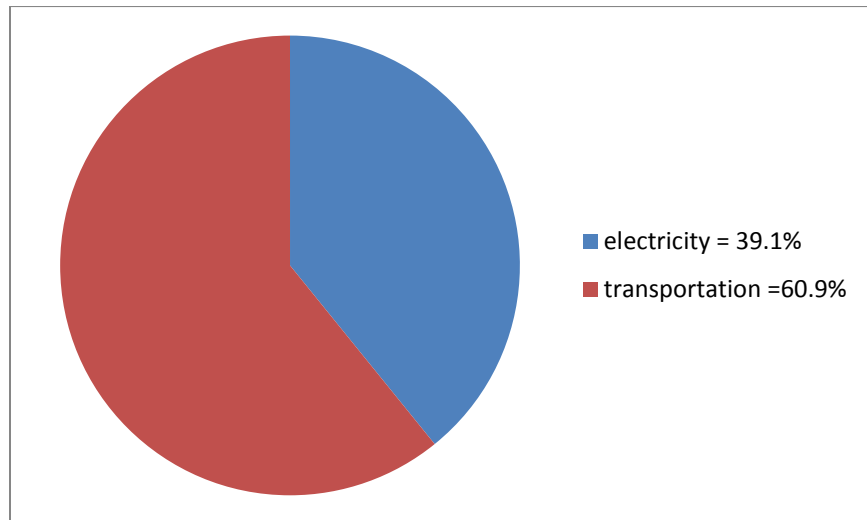


Fig. 16. TSGA system operating cost breakdown for the 10-mile scenario.

A breakdown of LCOSE of the TSGA system is given by percentage in Fig. 17 and by costs in Table 9. It appears that the contributions of the initial costs (for purchasing the absorption chiller, circulation pumps, cooling towers, working fluid, and the trailer tanks) to LCOSE are low—the combined contribution of the initial costs is only about 22%. The operating costs (i.e., the transportation and electricity costs) are more significant contributors to LCOSE. Reducing these costs is thus crucial to reduce LCOSE.

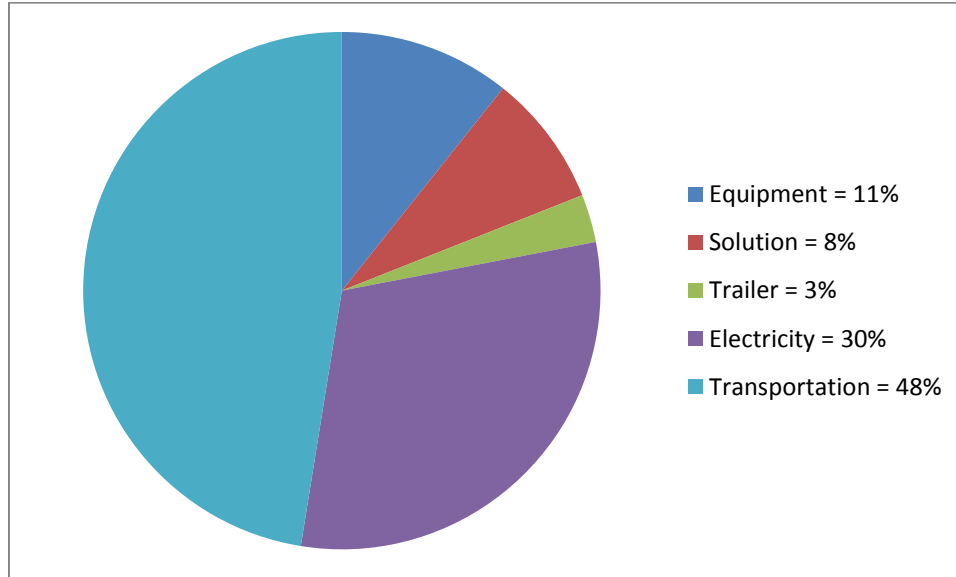


Fig. 17. Levelized cost breakdown of the TSGA system of the 10-mile case.

Table 9. Levelized cost breakdown of the TSGA system

	Item	Cost (\$)	Levelized cost (\$/kWh)
Capital cost	Equipment	374,703	0.0140
	Solution	\$289,845	0.0109
	Trailer tanks	\$105,000	0.0039
Operating cost	Electricity	71,887	0.0399
	Transportation	111,669	0.0620
Total levelized cost			0.1307

The LCOSE of this case is \$0.1307/kWh. It is higher than the cost of electricity in Houston area (\$0.102/kWh), which came with the large office building benchmark model and is used in the economic analysis of this study. However, the electricity price in Houston has varied moderately over the past a few years. For example, it went up to \$0.129/kWh in 2014 but dropped to \$0.107/kWh in 2015⁹.

4.3.2 Sensitivity Analysis

A series of sensitivity analyses were carried out to investigate the impact of various variables on the economics of the TSGA system. These variables include the distance between the geothermal site and the building, energy density of the TSGA system, electricity price, carrier cost for transporting the solution, and price of the solution.

⁹ http://www.bls.gov/regions/midwest/data/averageenergyprices_selectedareas_table.htm

4.3.2.1 Impacts of distance and building size

Distance between the geothermal site and the building affects the transportation cost, which accounts for around 61% of the TSGA system's annual operating cost in the 10-mile distance scenario. Meanwhile, with the increased distance, it takes more time for tanker trucks to travel between the two sites, and thus more trucks and working fluid would have to be brought in to maintain continuous cooling operation at the building. It thus increases both the initial and operating costs of the TSGA system.

Figure 18 shows the trend of both the electricity and transportation components of the annual operating cost of the TSGA system versus distance between the building and geothermal sites. The electricity cost, a little over \$71,000/year for running pumps and cooling towers, is not influenced by the distance, while the transportation cost (paid to the carrier supplier) increases linearly with the distance. From 5 miles to 20 miles, the transportation cost rises from \$69,700 (slightly less than the electricity cost) to around \$195,000 (2.7 times the electricity cost).

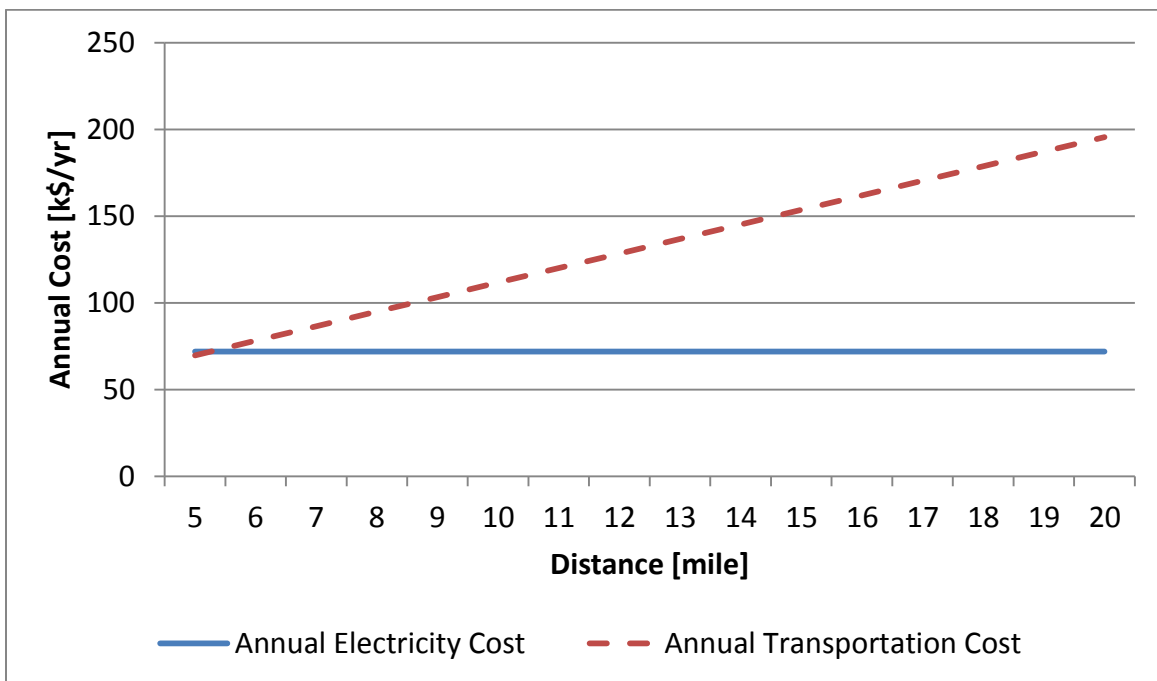


Fig. 18. Annual operating cost components vs distance.

Figure 19 shows the simple payback period for buildings of different sizes (and thus different annual cooling loads) versus distance from the geothermal site. Applying the TSGA system in larger buildings would result in shorter payback periods because savings in the operating cost increase more than the capital cost with the increase of the building size. Figure 19 also shows that the payback period increases with longer distance. As shown in Fig. 19, applying the TSGA system in buildings with large or double-large (e.g., district system) sizes yields payback periods shorter than 11 years if the building is within 10 miles of the geothermal site. However, the payback for applications in large buildings will be more than 20 years if the distance increases to 15 miles because the transportation cost increases proportionally with the increase in distance, as shown in Fig. 18.

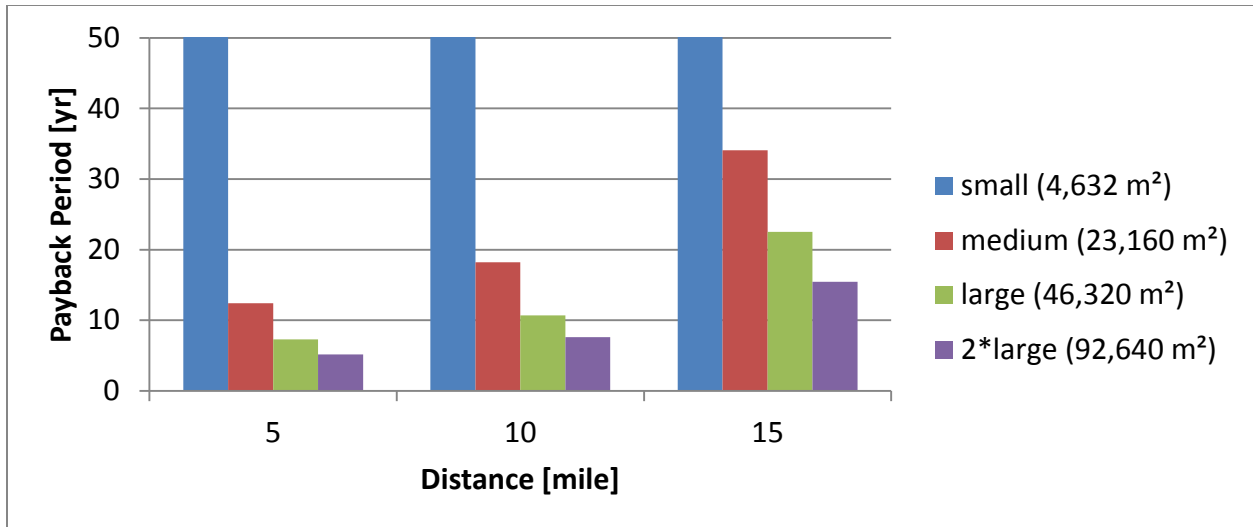


Fig. 19. Simple payback periods resulting from different building sizes and distances.

4.3.2.2 Impacts of transportation cost, electricity rate, and solution price

Transportation cost is determined by the distance and the carrier cost. In the 10-mile distance scenario, the carrier cost is \$52.2/hour, which is calculated based on the national average carrier cost (Fender et al. 2013) and the travel distance during one hour according to the truck operation schedule described in Appendix C. Figure 20 shows the change of payback resulting from a $\pm 10\%$ fluctuation in the carrier cost.

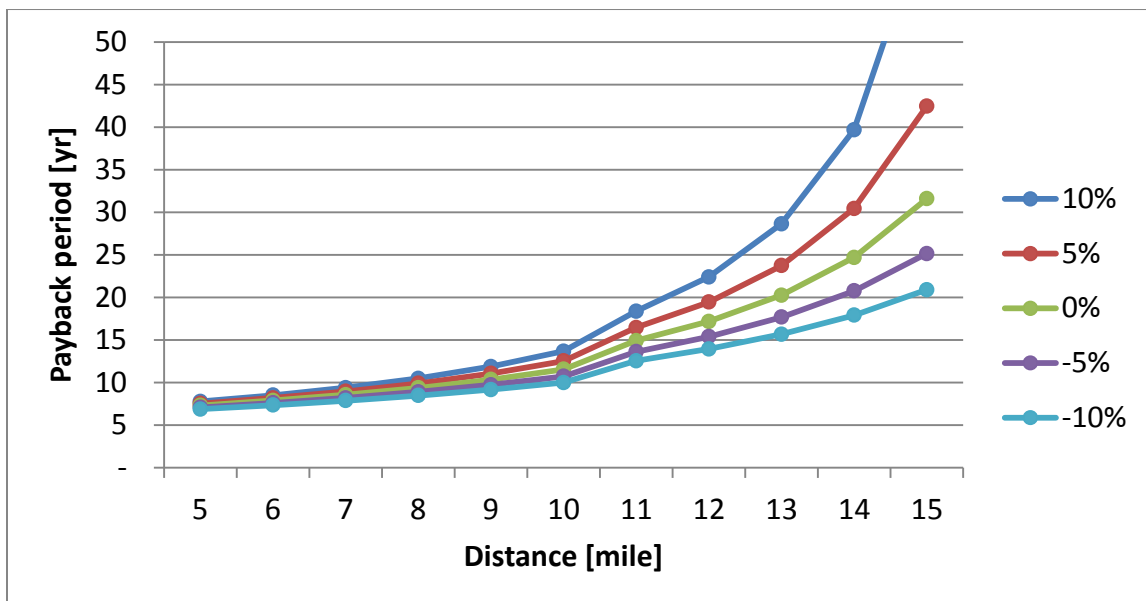


Fig. 20. Simple payback against fluctuation of carrier cost.

As shown in Fig. 20, for the same distance, a higher carrier cost leads to a longer payback period. Furthermore, the influence of carrier cost becomes more significant when the building is far from the geothermal site. With a 10-mile distance, the $\pm 10\%$ variation in the carrier cost leads to only about a 3.5 year difference in the payback period. However, the same variation leads to a 21 year difference (from 18 to 39 years) for a 14-mile distance.

A small jump in the payback period between 10 and 11 miles can be observed in Fig. 20. This jump is caused by an increase in the capital cost for purchasing one more truckload of working fluid in order to maintain continuous operation of the absorption chiller during the longer transportation course.

Figure 21 shows the impact of up to a $\pm 10\%$ variation in the electricity rate on the payback period at various distances. As shown in Fig. 21, a higher utility rate helps shorten the payback period, especially when the distance between the two sites is long. Compared with conventional vapor compression chillers, the TSGA system saves electricity, so higher electricity rates mean more savings in operating costs, which leads to shorter payback periods. The variation in electricity rate tends to affect the payback period more significantly at longer distances. The higher transportation costs that result from the longer distances offset much of the electricity cost savings and leave the total operating cost saving a rather small number. On the other hand, the initial cost premium of the TSGA system is not affected. As a result, a change in electricity rate results in a more drastic change in the payback period when the distance is longer.

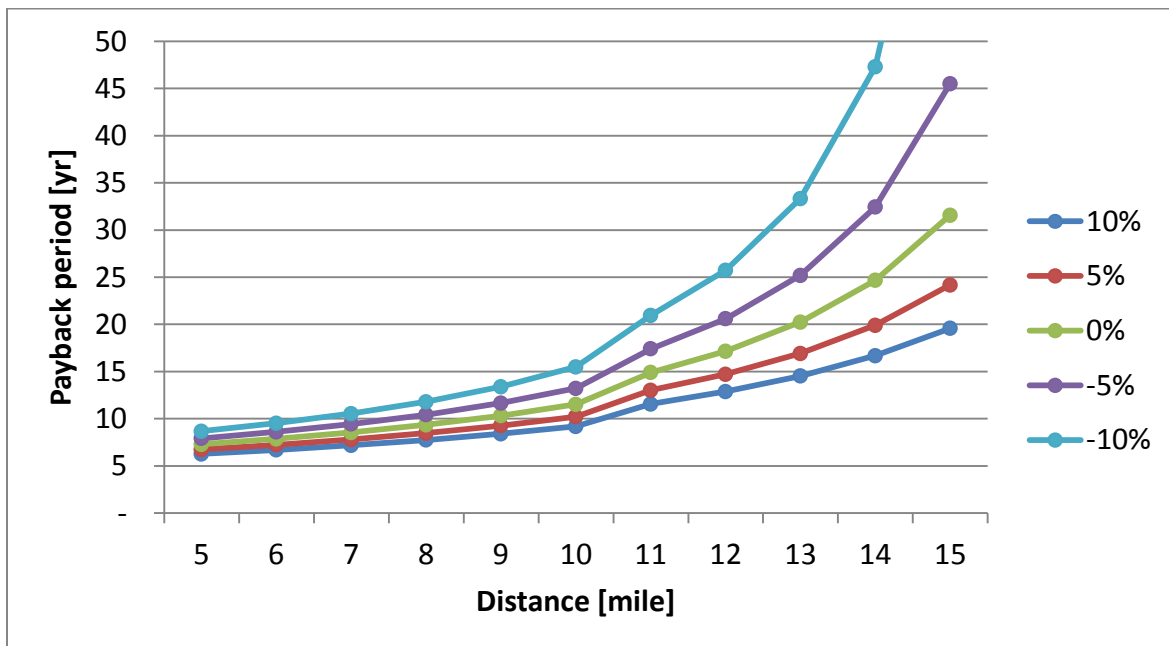


Fig. 21. Simple payback period against fluctuation of utility rate.

Figure 22 shows the impact of up to $\pm 20\%$ fluctuation in solution price on the payback period. Compared with the carrier cost and electricity rate, the solution price has moderate impact (less than 10%) on the payback period. This can be explained by the capital cost breakdown shown in Figure 15, where solution cost accounts for about one-fourth of the total capital cost. Thus, a 20% change in solution price only leads to a 5% change in the total capital cost.

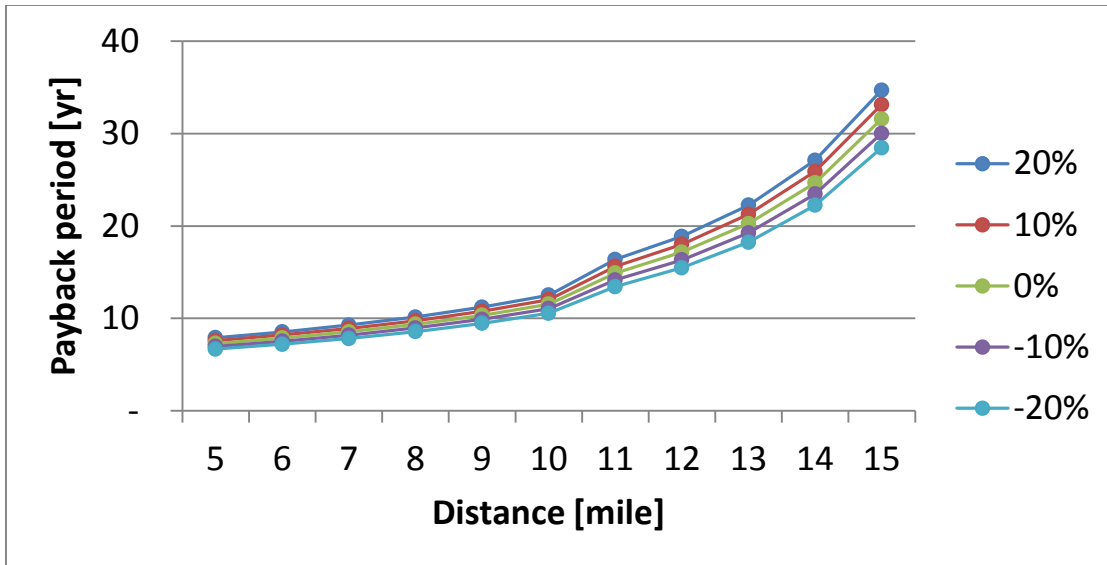


Fig. 22. Simple payback period against solution price.

4.3.2.3 Levelized cost

The LCOSEs of the TSGA system with a distance from 5 miles up to 20 miles and the breakdown of the LCOSEs are shown in Figure 23.

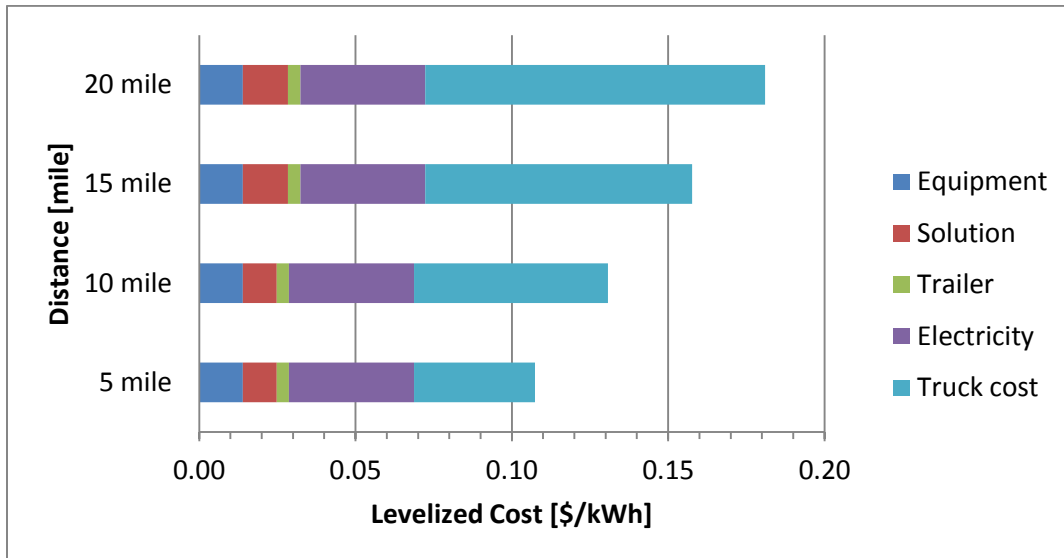


Fig. 23. Levelized cost breakdown for different distances.

The LCOSE increases with the distance between the building and the geothermal site. As shown in Figure 23, transportation cost increases linearly with the distance. The other costs are unaffected, except that the levelized cost of the solution increases by a small amount when the distance increases from 10 miles to 15 miles due to an increase in the amount of the working fluid for continuous operation of the TSGA system.

4.4 DISCUSSIONS

Two possible approaches to shorten the payback of the TSGA system are discussed, including (1) use of alternative transportation methods, such as pipeline or railway instead of tanker trucks, and (2) improving the solution energy density so that less transportation is needed.

4.4.1 Transportation Alternatives

There are two alternative transportation means to move large quantities of fluid instead of tanker trucks: pipeline and railway. In this section, the advantages, cost-effectiveness, and limitations of these two alternatives are briefly discussed.

4.4.1.1 Pipeline

Pipeline is a mainstream transportation method for many applications where a large quantity of fluid needs to be transported. It comes with the advantage of continuous operation and a relatively low operating cost. However, a pipeline application is limited by the large capital investment it requires and possibly by the complicated process to acquire the rights of way (ROWs) to dig trenches and install the pipes. In this section, the transportation cost associated with the pipeline option is calculated and is compared with the cost of using tanker trucks to transport the working fluid.

High density polyethylene (HDPE) pipes are assumed to be used for the pipeline, given their significantly lower cost compared with other pipe materials and their chemical compatibility with the LiBr/H₂O fluid pair. The cost of a pipeline (including two pipes: supply and return) for transporting the working fluid over a 10-mile distance is calculated with and without considering the ROW expenses. Details of the pipeline cost calculation are given in Appendix D. The calculated capital and annual operating costs of the pipeline option are listed in Table 10 along with that resulting from using tanker trucks.

Table 10. Comparison between the costs of using pipeline and tanker trucks for transporting working fluid over a distance of 10 miles

Option	Pipeline		Tanker truck
	Without ROW ^a	With ROW ^a	
Solution cost (\$)	833,310	833,310	289,845
Pipeline material and installation cost (\$)	357,500	357,500	-
Right-of-way (ROW) cost (\$)	0	1,056,000	-
Equipment cost (\$)	108,000	108,000	105,000
Total capital cost (\$)	1,298,810	2,354,810	394,845
Annual transportation cost (\$/year)	40,500	40,500	111,669
Life time cost for 20 years (\$)	2,108,810	3,164,810	2,628,225

^a ROW: right of way cost, which is estimated to be \$1/ft/year for 20 years.

As shown in Table 10, the solution cost of pipeline is higher than that of the tanker truck option because a large amount of solution is needed to fill the pipes. Equipment used for the pipeline option includes only pumps to circulate the working fluid through the pipeline. The equipment for the tanker trucker option only includes three trailer tanks. The tanker trucks are rented, and the rental cost is included in the annual transportation cost. When ROW is not considered, the total capital cost (including solution, pipeline, and equipment) of the pipeline option is more than three times of that of the tanker truck option. ROW cost varies widely, depending on the types of land that the pipeline will pass through. We estimated the ROW

cost to be \$1/ft/year for the size of the pipeline that was used in the case study. That cost is the average of ROW costs found in various resources^{10,11,12,13}. With the estimated ROW cost, the total capital cost of the pipeline option is six times of that of the tanker truck option. However, the annual operating cost of a pipeline (for running the circulation pumps to deliver the needed amount of working fluid to satisfy the fluctuating cooling load of the building) is less than half of the operating cost of the tanker trucks. When the ROW cost is accounted for, the lifetime cost (including the total capital cost and the cumulative transportation cost for 20 years) of the pipeline option is 20% higher than that of the tanker truck option.

Figure 24 shows the simple payback periods of the TSGA system resulting from the two transportation options for various distances. The payback period with the pipeline option increases almost linearly with the increase of distance. In contrast, the payback period with the tanker truck option is relatively flat for a short distance but increases drastically for distances more than 15 miles because more tanker trucks are needed then to keep the TSGA system in continuous operation. Without accounting for the ROW cost, the two options result in similar payback periods for a distance less than 13 miles. However, when the ROW cost is accounted for, the pipeline option results in longer payback periods than the tanker truck option when the distance is more than 3 miles but less than 17 miles. To get a payback period of less than 20 years, the distance for pipeline cannot be more than 10 miles. For very short distances (< 3 miles), pipeline is more cost effective than the tanker trucks.

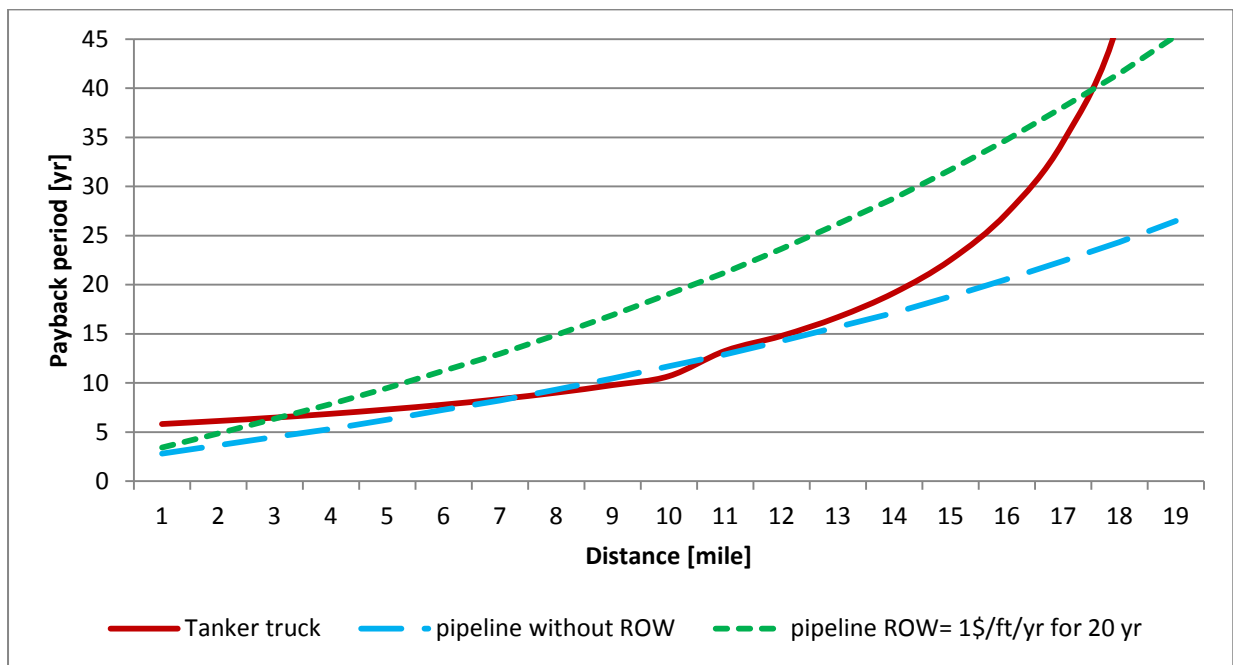


Fig. 24. Total cost comparison between pipeline and truck for a distance of 10 miles.

4.4.1.2 Railway

Railway has always been a cost-effective method to transport large quantities of cargo, including fluid, over long distances. However, transporting by rail is hindered by availability. Only locations with access to a railway that has a suitable operating schedule can take full advantage of this transportation method. In addition, a special freight car made with plastic would be needed to transport the LiBr/H₂O solution.

¹⁰ Source: www.in.gov/idoa/files/easement_Policy.doc

¹¹ Source: http://www.dcnr.pa.gov/cs/groups/public/documents/document/dcnr_003536.pdf

¹² Source: http://www.wvsoro.org/resources/advice/Pipelines_What_Surface_Owners_Should_Know_2014-08-27.pdf

¹³ Source: <http://extension.psu.edu/natural-resources/natural-gas/news/2010/04/pipelineinfo>

When a railway is accessible, it is likely that the transportation cost could be reduced by combining railway and tanker truck (or pipeline for short distance).

4.4.2 Enhanced TSGA System

The energy density of the TSGA system can be improved by raising the strong solution concentration and/or by reducing the weak solution concentration. The strong solution cannot be made so strong that it exceeds the crystallization limit of the LiBr/H₂O solution.

A series of simulations were carried out to investigate the possible operating performance of the TSGA system using the ORNL SorpSim software. For the current design, the TSGA system operates between 53% and 62% concentrations, as shown in Fig. 25, yielding an energy density of 150 Btu_{clg}/lb (0.097 kWh_{clg}/kg). As shown in Fig. 25, the 62% concentration line is parallel with the crystallization line when temperature drops below 50°C (122°F), which indicates a very low risk of crystallization (Liao and Radermacher 2007).

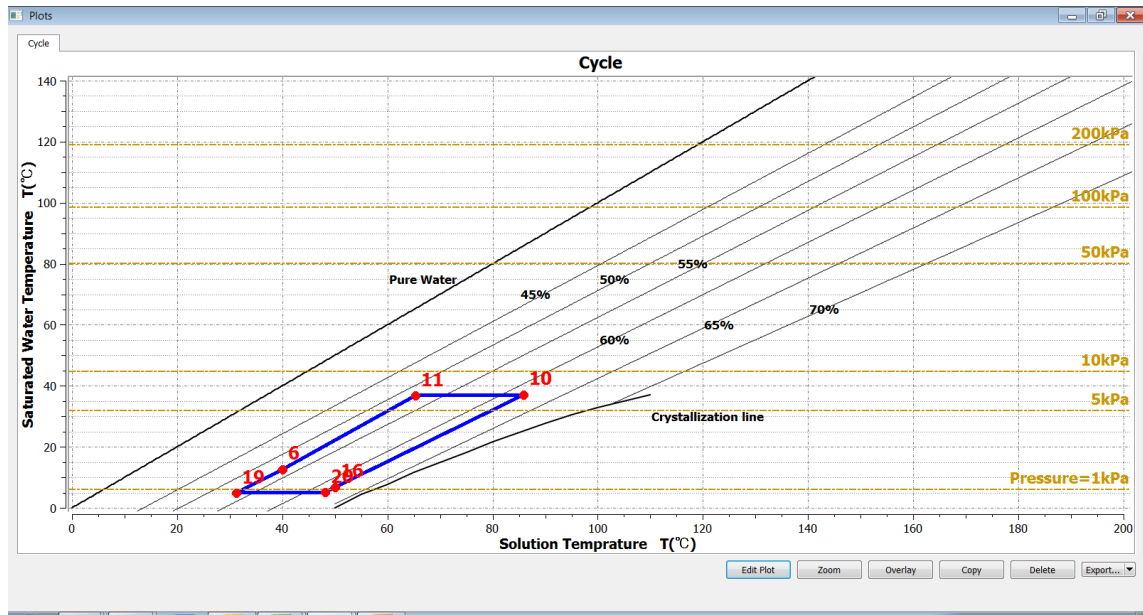


Fig. 25. Current TSGA operation on Dühring chart.

If the strong solution concentration is increased to 65% by reducing the solution flow rate, it yields an energy density of 155 Btu_{clg}/lb (0.1 kWh_{clg}/kg), or a 3% increase compared with the current design. However, as shown in Fig. 26, the strong solution process line is very close to the crystallization line, and it is likely to crystallize once the temperature drops below 50°C (122°F). Since the strong solution needs to be transported in tanker trucks and stored in large tanks before entering the absorber in the building, it is likely that the temperature will drop below 30°C and the crystallization will happen. Thus, a higher concentration for better energy density is not an option for the strong solution due to the high risk of crystallization.

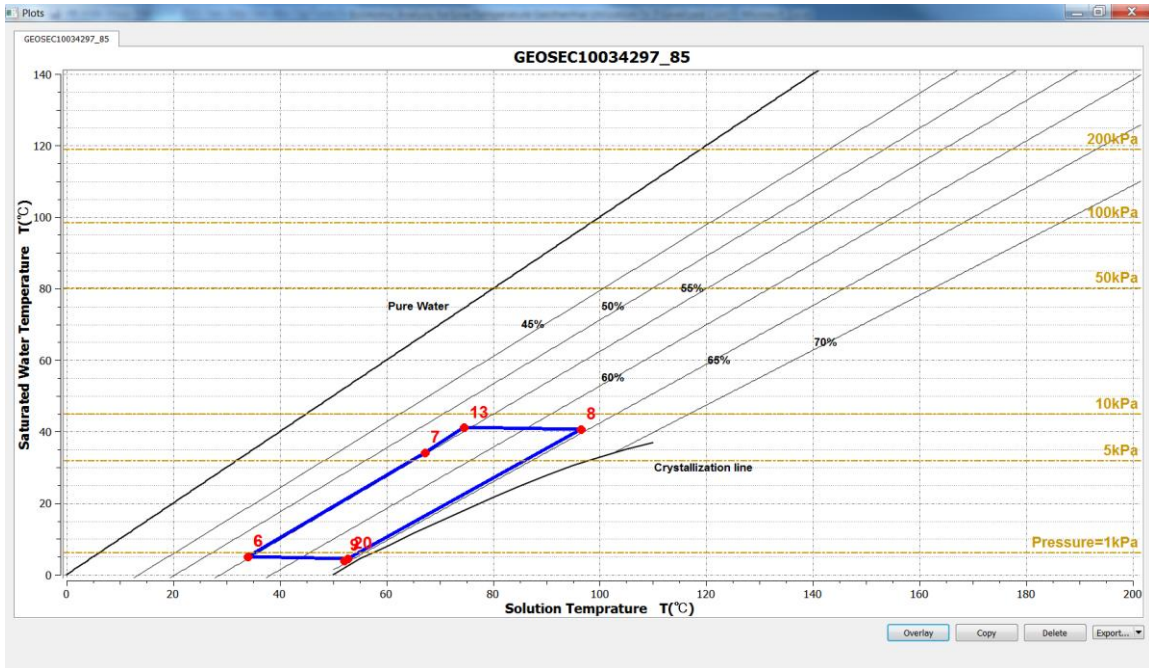


Fig. 26. Modified TSGA operation with higher concentration on Dühring chart.

The other approach to achieving higher energy density is to reduce the weak solution concentration by increasing the evaporating temperature at the evaporator. However, a high evaporating temperature will either be unable to provide the required 45°F (7.2°C) chilled-water temperature or will result in a large decrease in cooling capacity due to the reduced temperature difference in the evaporator.

One approach to reduce the evaporating temperature is to deal separately with the sensible and latent cooling loads of the building using a cascaded process. As shown in Fig. 27, the strong solution generated at the geothermal site will go through a dehumidifier and will absorb the moisture in the outdoor air before it enters the absorber for making the chiller water. Since most of the latent cooling load of the building is from outdoor air ventilation, which has been dehumidified with the strong solution, the chilled water is only needed to deal with the sensible cooling load, and the evaporating temperature can thus be elevated to 54°F (12.2°C).

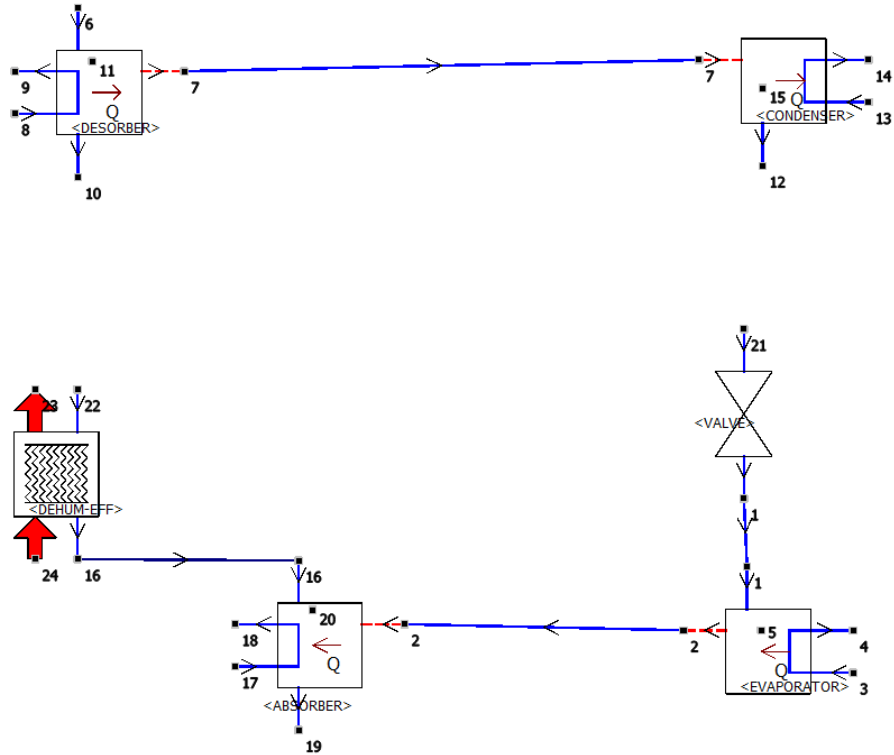


Fig. 27. An example of TSGA dehumidification hybrid system.

With the chilled-water temperature increased from 45°F (7.2°C) to 54°F (12.2°C), the absorption cycle operates with the solution concentration between 51.7% and 61.8%, which yields an energy density of 0.11 kWh_{clg}/kg_{WS}, resulting in a 12.8% decrease of the required amount of the working fluid.

However, such a cascaded system comes with a price: with separate sensible and latent loads, the supply air temperature is increased because of the higher chilled-water temperature. This leads to a smaller temperature difference between the indoor space and the supply air; thus a larger amount of air circulation needs to be supplied. As a result, a larger duct system or more fan power will be needed for the building's cooling system.

5. CONCLUSIONS AND RECOMMENDATIONS FOR FUTURE WORK

Low-temperature geothermal resources [lower than 150°C (300°F)] are abundant in the United States. They exist in the western states at shallow depths and in most other parts of the country at depths of 3 km (9,842 ft). In addition, oil and gas production in the South and the Midwest also coproduce water at temperatures higher than 80°C (176°F). These low-temperature geothermal resources can be used to provide heating and cooling to buildings. With absorption or adsorption technologies, low-temperature geothermal energy near buildings has been successfully used to provide space cooling and refrigeration in the United States and other countries. These geothermal absorption cooling systems can reduce fossil fuel consumption, peak electric demand, and the use of refrigerants with high potentials for global warming and ozone depletion.

However, low-temperature geothermal energy remains underutilized. The typically long distances between geothermal sources and potential end uses and the low density of the transported thermal energy are key barriers preventing its wider use. For existing operational geothermal installations providing thermal end uses, the geothermal resource is either at the demand site or within a 2-mile distance.

ORNL proposed an innovative two-step absorption technology, referred as two-step geothermal absorption (TSGA) system. With TSGA, the low-temperature geothermal energy is stored in a LiBr/H₂O solution and transported at ambient temperature, with a significantly higher energy density than the conventional way of transporting hot water. The technical challenges identified include (1) reducing required volume (i.e. increasing energy density) and cost of the working fluid, (2) harvesting heat from sparsely located geothermal wells with varying production rates, (3) maintaining appropriate vacuum levels for various components of the two-step absorption cycle, and (4) retaining the quality of the working fluid during transportation and storage.

A conceptual design of the TSGA system was developed based on the single-effect absorption cycle. LiBr/H₂O solution was selected as the working fluid pair due to its superior performance over other candidate fluid pairs. Key design parameters of a 900 ton two-step absorption chiller were determined based on computer simulations of the proposed system. The simulations predict that the two-step absorption chiller has an annual average COP_{th} of 0.67, and the energy density of the transported solution is 150 Btu_{clg}/lb (0.097 kWh_{clg}/kg) (i.e., providing 150 Btu of cooling per pound of shipped LiBr/H₂O weak solution).

A case study for applying the TSGA system to a large office building at Houston, Texas, was conducted with available data in several related disciplines (e.g., the characteristics of the low-temperature geothermal resources, the demands for space cooling, and available methods for transporting the stored geothermal energy to the demand site). This case study indicates that for a distance of 10 miles from the geothermal site to the building, the simple payback of the investment on the TSGA system is 10.7 years when compared with the conventional minimum code-compliant electric-driven vapor compression chiller. It indicates that the TSGA system can provide space cooling to buildings 10 miles away from the geothermal resources, and such applications would be economically competitive with other advanced electric-driven vapor compression chilling technologies.

A series of sensitivity studies were conducted to investigate the sensitivity of the economics of the TSGA system to various design parameters. The economics were found to be highly sensitive to the distance, building size (cooling loads), transportation carrier cost, and the electricity rate, but less sensitive to the price of the working fluid. The largest component of the LCOSE for the TSGA system is the cost for transporting the working fluid back and forth between the geothermal site and the building.

In addition to the tanker truck option, rail and pipeline transportation were investigated. For a distance of 10 miles, the tanker truck option has a lower life cycle cost than a pipeline using HDPE material over a 20 year period. Railway transportation may have a lower operating cost than the tanker truck option, but it is limited by the accessibility to the railway stations. A hybrid means of transportation combining both the railway (for long distances) and the tanker truck (for short distances) may help reduce the transportation cost.

The amount of working fluid that must be transported can be reduced by integrating an absorption-based dehumidifier into the proposed TSGA system in a cascade configuration. Since the sensible and latent cooling are dealt with separately, the chilled-water temperature can be elevated, which leads to an greater difference in concentration between the strong and weak solutions of the working fluid and therefore an increase in energy density of the transported fluid.

REFERENCES

- American Petroleum Institute (API). 2006. "Where does the U.S. produce oil and natural gas?" Accessed online at <http://www.api.org>.
- ASHRAE, A. S. 2004. Standard 90.1-2004, Energy standard for buildings except low rise residential buildings. American Society of Heating, Refrigerating and Air-Conditioning Engineers, Inc.
- Boyd, T. 2015. Direct Uses in the U.S. Retrieved August 28, 2015, from <http://energy.gov/eere/geothermal/direct-use-geothermal-workshop-summary#0-2>.
- Carlson, S., 2001, "Develop Full Load Heating and Cooling Hours for GCHPs Applied in Various Building Types and Locations". ASHRAE Research Report RP-1120. American Society of Heating, Refrigerating and Air Conditioning Engineers, Atlanta, GA.
- Clark, C. and J. Veil. 2009. Produced Water Volumes and Management Practices in the United States. Environmental Science Division, Argonne National Laboratory. Available at <http://www.ipd.anl.gov/anlpubs/2009/07/64622.pdf>.
- Conde-Petit, M. R. 2014 *Aqueous solutions of lithium and calcium chlorides: Property formulations for use in air conditioning equipment design*. M.Conde Engineering. Available at <http://www.mrc-eng.com/Downloads/Aqueous%20LiCl&CaCl2%20Solution%20Props.pdf>
- Deru, Michael, et al. 2011. "US Department of Energy commercial reference building models of the national building stock." (2011): 1.
- DOE. 2015. "Direct Use of Geothermal Energy." Available at <http://energy.gov/eere/geothermal/direct-use-geothermal-energy>.
- DOE. 2004. *Buried Treasure: The Environmental, Economic, and Employment Benefits of Geothermal Energy*. Geothermal Technologies Program. DOE/GO-102004-1985. Revised in November 2004.
- European Geothermal Energy Council (EGEC). 2005. *Key Issue 5: Innovative Applications Geothermal Utilisation for Cooling*. Available at http://www.erec.org/fileadmin/erec_docs/Projcet_Documents/K4_RES-H/K4RES-H_Geothermal_cooling.pdf.
- Fender, Katherine J., and Pierce, David A. 2013. *An analysis of the operational costs of trucking: a 2013 update*. American Transportation Research Institute.
- GHC (Geo-Heat Center). 2005. Geothermal Direct-Use Case Studies. Website: <http://geoheat.oit.edu/casestudies.htm>. Accessed: June, 23, 2008.
- Grossman G. 1998. ABSIM: Modular Simulation of Absorption Systems. ORNL/Sub/86-XSY123V
- Holdmann G. 2005. "Geothermal Powered Absorption Chiller." Presented at the 2005 Rural Energy Conference, Valdez, Alaska, September 20, 2005.
- Interstate Oil and Gas Compact Commission and ALL Consulting (IOGCCAC). 2006. *A Guide to Practical Management of Produced Water from Onshore Oil and Gas Operations in the United States*. Available at https://fracfocus.org/sites/default/files/publications/a_guide_to_practical_management_of_produced_water_from_onshore_oil_and_gas_operations_in_the_united_states.pdf.
- Jiang, Yi, Xie, Xiaoyun. 2015. "Absorption heat exchangers for long distance heat transportation," ICR 2015, August 16–22, Yokohama, Japan.
- Kreuter H. 2012. "Geothermal Applications: Geothermal Cooling." Proceedings of the Renewable Energy Training Program, 10 July 2012, ESMAP – IFC, Washington, DC.

- Lech, P. 2009. *A New Geothermal Cooling – Heating System for Buildings*. Master’s Thesis. University of Iceland and the University of Akureyri.
- Liao, X. and Radermacher, R. 2007. Absorption chiller crystallization control strategies for integrated cooling heating and power systems, Technology Research Center, January 2007.
- Lienau, P. 1996. “OIT geothermal system improvement.” *Geothermal Resources Council Transactions*, Vol. 20, September/October 1996.
- Lund, J. Industrial Applications. Retrieved August 28, 2015, from <http://energy.gov/eere/geothermal/direct-use-geothermal-workshop-summary#0-2>
- Luo et al. 2010. “An Absorption Refrigeration System Used for Exploiting Mid-low Temperature Geothermal Resource.” *Proceedings World Geothermal Congress 2010*, Bali, Indonesia, 25–29 April 2010.
- Manuel R. Conde-Petrit. 2009. “Aqueous solution of lithium and calcium chlorides for use in air conditioning equipment design M.,” CONDE ENGINEERING.
- National Research Council (US). 2010. Committee to Assess Fuel Economy Technologies for Medium- and Heavy-Duty Vehicles. *Technologies and Approaches to Reducing the Fuel Consumption of Medium-and Heavy-Duty Vehicles*. National Academies Press.
- Nordquist, J. 2009. “Geothermal Power Plant Technologies.” Ormat Technologies, Inc.
- Reed Construction. 2010. "RS Means Mechanical Cost Data 2010." Kingston, MA.
- Storch, G., & Hauer, A. 2006. “Cost-effectiveness of a heat energy distribution system based on mobile storage units: two case studies.” In Proceedings of the ECOSTOCK conference, Stockton.
- USGS (United States Geological Survey). 2015. Produced waters database (accessible via <http://energy.cr.usgs.gov/prov/prodwat/>).
- Wang et al. 2013. “Application of geothermal absorption air-conditioning system: a case study.” *Applied Thermal Engineering* 50, 71–80.
- Williams C. 2013. National Geothermal Resources Assessment and Classification. Presentation for Geothermal Technologies Program 2013 Peer Review. April 24, 2013 (available at http://energy.gov/sites/prod/files/2014/02/f7/g_s_resource_assessment_peer2013.pdf).

APPENDIX A. FURTHER INFORMATION ON TSGA SYSTEM

A-1. GEOTHERMAL SITE COMPONENTS

- **The assembly of desorber and condenser** is a partial vacuum container with two sections. Heat from the geothermal fluid boils off water from the LiBr/H₂O solution at the desorber (at the bottom section of the assembly). The water vapor is then condensed by a heat exchanger at the condenser (at the top section of the assembly). The solution is circulated between a tanker and the desorber until the solution is concentrated to the desired level (usually not higher than 65% to avoid crystallization). The required temperature level at the desorber is governed by the properties of the LiBr/H₂O solution and the cooling water temperature at the condenser. For a typical single-effect absorption cycle using an LiBr/H₂O solution, the heat supplied to the absorber typically shall have a temperature above 90°C (194°F). The cooling water temperature at the condenser, which determines the water vapor pressure in the assembly, depends on the type and operation of the cooling tower. The typical design cooling water temperatures is 29°C (85°F) if a wet-cooling tower is used, and it will be higher if a dry cooler is used. Given the operating temperature range, the heat exchanger inside the assembly can be made with carbon steel and copper. If the quality and chemistry of the geothermal fluid is good enough (i.e., clean and without risk of corrosion), the geothermal fluid can be routed directly into the heat exchanger. However, if the quality of the geothermal fluid is a concern, an intermediate heat exchanger shall be used to separate the geothermal fluid from the heat exchanger in the assembly. The intermediate heat exchanger shall be made with copper-nickel alloys or other similar materials that are highly resistant to corrosion in salty water.
- **A cooling tower** is used to condense the water vapor in the assembly to liquid water and thus maintain the low pressure in the assembly. Depending on availability of makeup water, either a wet or dry cooling tower can be used. The cooling water provided by a dry cooler will be warmer than that from a wet cooler. As a result, the pressure in the absorber and condenser assembly will be higher and the required minimum temperature of the geothermal fluid will also be higher.
- **A cooling tower circulation pump** is used to circulate cooling water between the condenser and the cooling tower. In addition, if an intermediate heat exchanger is used, another circulation pump is needed to circulate a heat carrier fluid between the absorber and the intermediate heat exchanger.
- **A geothermal fluid pump** is used to draw geothermal fluid from existing piping and push it through the heat exchanger in the desorber then back to the geothermal fluid piping.

A-2. BUILDING SITE COMPONENTS

- **The assembly of absorber and evaporator** is another partial vacuum container, which has lower pressure than the assembly of desorber and condenser. It also has two sections. The concentrated solution is throttled through a flow restrictor and then sprayed into the absorber (at the top section of the assembly), where it absorbs water vapor from the evaporator (at the bottom section of the assembly). To continue the absorption process, the absorber is cooled by the water flow from a cooling tower. In a similar fashion, pure water in liquid form is throttled through another flow restrictor and sprayed into the evaporator, where it is evaporated, due to the low pressure created by the absorber, and extracts heat from the chilled water system of the building. The pressure in this assembly is determined by the vapor pressure characteristics of the LiBr/H₂O solution. To produce the 7°C (45°F) chilled water typically required for space cooling, the liquid water needs to be evaporated at about 5°C (41°F), and the corresponding water vapor pressure is 0.872 kPa (0.009 atm). This low-pressure requirement makes the absorption process is very sensitive to air leakage and the existence of nonabsorbable gases because air and other gases not only degrade absorption

performance but also accelerate corrosion in the assembly. It is thus critical to keep a hermetic environment in the assembly, and a vacuum pump is needed to purge air and other gases out of the assembly.

- **Flow restrictors** are used to reduce the pressure of the liquid water and the concentrated solution before they enter into the evaporator and the absorber, respectively. The flow restrictor can also be used to modulate the flow rates of the concentrated solution and the water so that the cooling capacity of the evaporator can be varied to satisfy the fluctuating cooling demand of the building.
- **A wet cooling tower** is used to supply water flow to cool the absorber during the absorption process. Since the temperature of the cooling water determines the saturated concentration of the LiBr/H₂O solution at the near vacuum pressure inside the absorber, a wet cooling tower is needed to keep the cooling water temperature close to the wet bulb temperature of the ambient air.
- **A cooling tower circulation pump** is used to circulate cooling water between the absorber and the wet cooling tower. It is the same as that used for conventional absorption chillers.
- **Holding tanks** are used to temporarily store the concentrated solution transported from the geothermal site and the diluted solution discharged from the absorber. These storage tanks are made with rubber or polymer compounds that are compatible with the LiBr/H₂O solution. At least two tanks are needed: one is for the strong solution and the other is for the weak solution. An additional water tank is needed if the condensed water is also transported from the remote desorber and used in the evaporator. All these tanks shall be slightly pressurized with inert gas to prevent air leak.
- **A solution pump** is used to pump the diluted solution from the absorber, in which the pressure is near vacuum, to the holding tanks, in which the pressure is maintained slightly above the atmospheric pressure.

A-3. IMPACT OF WET OR DRY COOLING AT GEOTHERMAL SITE

A wet cooling tower can provide cooler fluid to the condenser than a dry cooler. As a result, if a wet cooling tower is used for the condenser, the two-step geothermal absorption chiller can have slightly (5%) larger capacity with smaller (10% to 20% less) UA values (i.e., size) for condenser and absorber (Table A-3.1). In addition, the solution efficiency can be increased by 6%. As shown in Fig. A-3.1, with wet cooling tower, the water vapor pressure at the desorber becomes lower (6.3 kPa) and the concentration of the solution is increased. It means, for the same temperature at absorber, the concentration differential between the strong and weak solution can be increased.

This comparison indicates that, to reduce the needed amount of LiBr/H₂O solution, the condenser at the geothermal site shall use a wet-cooling tower. However, the availability and quality of water at geothermal site may limit the usage of wet cooling tower.

Table A-3.1. Component size and performance of the two-step geothermal absorption chiller with different types of cooling tower for the condenser at geothermal site

	Dry cooling tower		Wet cooling tower	
	UA value (kW/°C)	HT (kW)	UA value (kW/°C)	HT (kW)
Evaporator	600	3189	600	3363
Internal heat exchanger	25	676.5	25	628.4
Desorber	425	4411	425	4581
Condenser	1000	3414	895	3599
Absorber	375	4186	305	4345
Thermal efficiency (%)	72		73	
Solution efficiency (kg/kWh)	12.6		11.9	

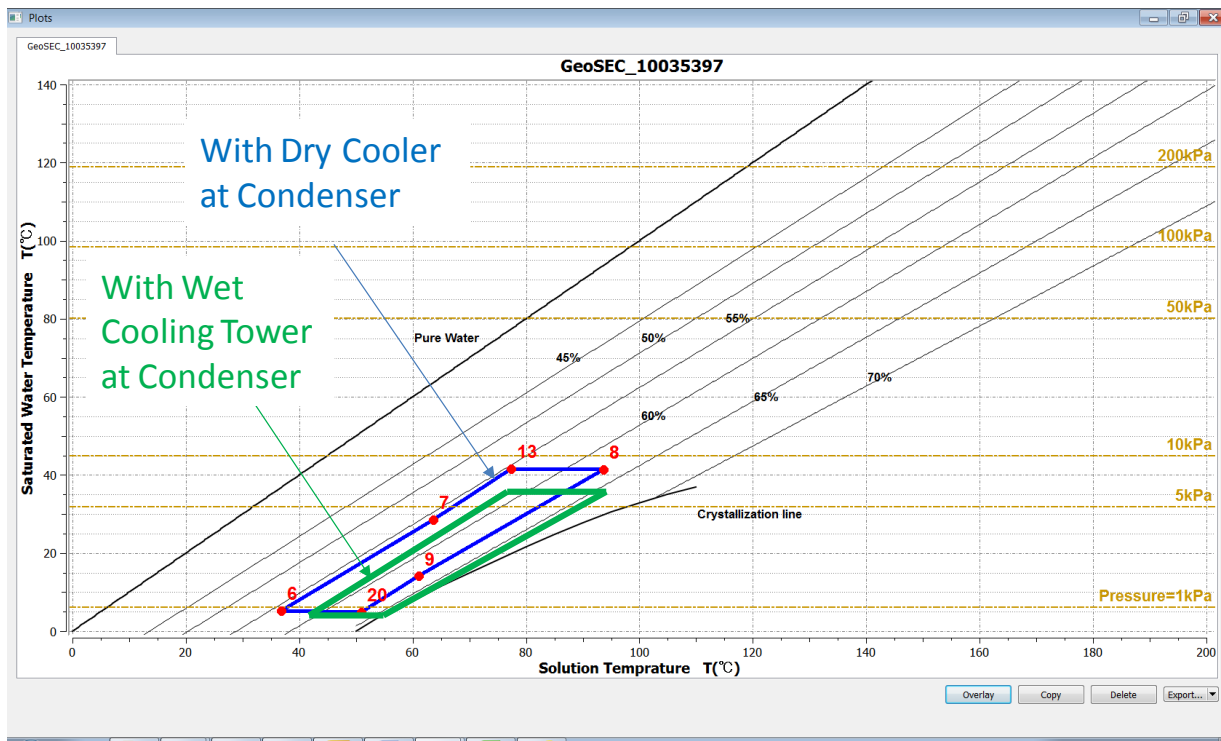


Fig. A-3.1. State points of two-step geothermal absorption cooling shown on Dühring chart for LiBr/H₂O—dry cooler vs. wet cooling tower for the condenser at geothermal site.

A-4. EFFECT OF GEOTHERMAL FLUID TEMPERATURE

Impacts of the geothermal entering fluid temperature (abbreviated as Geo-EFT) on the performance of the absorption cooling are investigated through computer simulations. The simulation-predicted performance of the geothermal absorption chiller with two different Geo-EFTs is listed in Table A-3.2. The simulated performance data indicate that when Geo-EFT drops down to 185°F (85°C) from 212°F (100°C), the cooling capacity of the chiller decreases by 37%, and the heat transfer rates at other components also decrease by 34–37%. Furthermore, the solution efficiency is reduced by 65%! As a result, the size of the components, flow rates of heat transfer fluids, and the amount of the LiBr/H₂O solution all need to be significantly increased to provide the same space cooling service to the building. Figure A-3.2 indicates that with the 185°F (85°C) Geo-EFT, the concentration differential of the solution is only 4%, which is

42% smaller than what it would be with 212°F (100°C) Geo-EFT. It means to provide the same amount of cooling energy, the required amount of LiBr-H₂O solution will be nearly doubled.

This comparison indicates that lower Geo-EFT results in smaller cooling capacity and lower solution efficiency. Therefore, geothermal resources with relatively higher temperature shall be used to reduce the cost of the two-step geothermal absorption system. However, on the other hand, when Geo-EFT is higher than 212°F (100°C), the LiBr-H₂O solution can be concentrated to a level high than 65%. It significantly increases the risk of crystallization, especially when the solution is later cooled down at other component of the system (e.g., during transportation and storage).

Table A-3.2. Component size and performance of the two-step geothermal absorption chiller with different entering fluid temperatures from geothermal source

Component design	212°F (100°C) Geo-EFT		185°F (85°C) Geo-EFT	
	UA value (kW/°C)	HT (kW)	UA value (kW/°C)	HT (kW)
Evaporator	600	3189	600	2018
Internal heat exchanger	25	676.5	25	570
Desorber	425	4411	425	2879
Condenser	1000	3414	1000	2137
Absorber	375	4186	375	2760
Thermal efficiency (%)	72		70	
Solution efficiency (kg/kWh)	12.6		20.8	

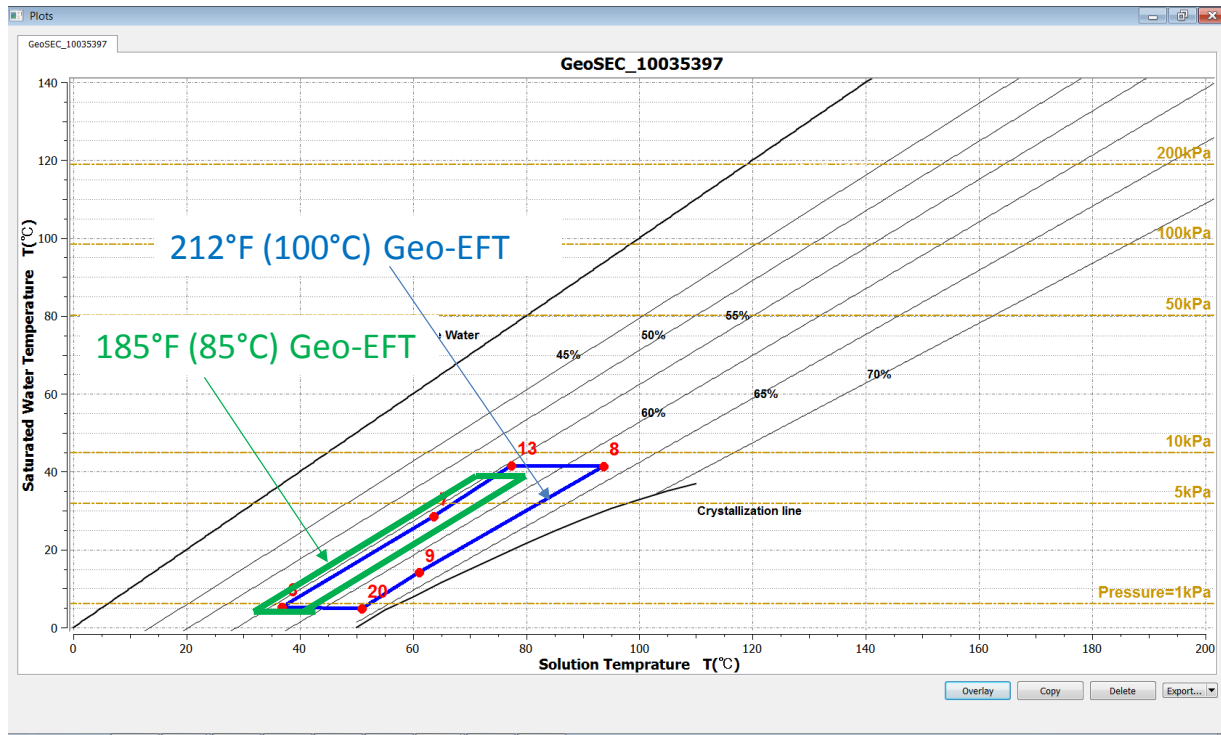


Fig. A-3.2. State points of two-step geothermal absorption cooling shown on Dühring chart for LiBr/H₂O— with different Geo-EFTs.

A-5. TRANSPORTATION REGULATIONS PERTAINING TO LiBr/H₂O Solution

The LiBr-H₂O solution is not hazardous as defined in 49 CFR 172.101 by the U.S. Department of Transportation. Shipments of LiBr-H₂O solution by water, rail, or truck are acceptable within each carrier's weight limits and packaging requirements. Tankers for transporting LiBr-H₂O solution are similar to those used for transporting other nonhazardous liquids and with following features. To ensure reliable operation of the TSGA system, the tanker shall have following features:

- Pressurized with inert gas to prevent air infiltration.
- At least two compartments in the tanker to store solution and pure water separately if the condensed water needs to be reused.

APPENDIX B. FITTING CORRELATIONS OF COMPONENT PRICE

The cost-size correlations are derived from data available in *RSMeans Mechanical Cost Data* (Reed Construction 2010). Table B-1 summarizes the correlation factors for different components and the data sources, based on which these correlation factors are derived.

Table B-1. Fitting correlations of component prices

Component	A	B	Source
Water-cooled vapor compression system	472.4	9047.4	RSMeans 23 64 16.10 centrifugal-type water chillers centrifugal, packaged unit, water cooled, not incl. tower 400 ton–1200 ton
Non-direct-fire absorption system	601.52	136117.8	RSMeans 23 64 13.16 indirect-fired absorption water chiller 250 ton–1125 ton
Pump	2.54	3316.3	RSMeans 23 21 23.13 close coupled, end suction, bronze impeller 150 gpm–1550 gpm
Cooling tower	88.63	12613	RSMeans 23 65 13.10 forced draft-type cooling towers, axial fan, induced draft, 500 ton–1000 ton

REFERENCES

Reed Construction. 2010. "RS Means Mechanical Cost Data 2010." Kingston, MA.

APPENDIX C. TRUCK OPERATION SCHEDULE

Figure C-1 illustrates the truck operation schedule for case with a 10-mile distance.

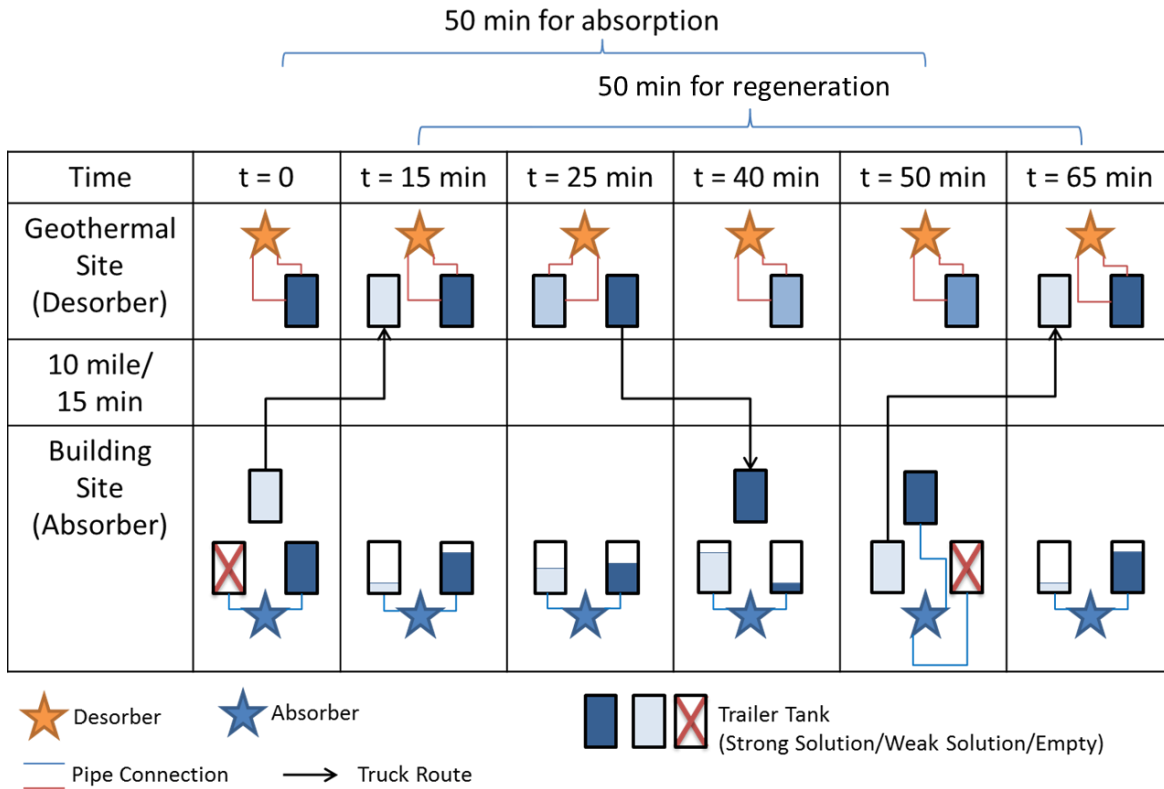


Figure C-1. Truck operation schedule at peak load condition.

As shown in Fig. C-1, there are two trailer tanks always at the building site: one is to supply strong solution and the other is to receive the weak solution. There is always one trailer tank at the geothermal site, which is connected with the desorber to regenerate the solution. For one-truck scenario, the fourth trailer tank is shipped by the tractor-truck to transport the weak solution from the building to the geothermal site, or the strong solution from the geothermal site to the building. The strong solution in one of the two trailer tanks at the building is piped into the absorber, and the weak solution is pumped into the other trailer tank.

At the peak load condition, once the tank holding the strong solution is emptied, and in the meanwhile, the tank holding weak solution is full, the third trailer tank full of strong solution would have just arrived. Then the source of strong solution is quickly switched,¹⁴ and the trailer full of weak solution is shipped by the tractor to the geothermal site. When it arrives at the geothermal site, solution in the fourth tank has already been fully regenerated. The trailers are then switched, and the tank holding the strong solution is shipped by the tractor back to the building while the newly arrived weak solution starts to be regenerated. Assuming it takes 10 min to switch the trailer tanks at either the building or the geothermal site, it will then take 50 min to complete a round trip: 20 min for switching trailer tanks and 30 min on the road to travel 20 miles.

¹⁴ To ensure a smooth transition, a small storage tank with multiple inlets for strong solution may be needed between the absorber and the trailer tanks.

During part load hours, the strong solution consumption rate is slower, thus when a new trailer tank full of strong solution arrives at the building, the previous strong solution trailer tank is not emptied yet. The tractor is thus not needed during the time between the arrival of the strong solution and departure of the fully filled weak solution trailer. If the tractor can be dismissed during this time period, the total operation/rental time of the truck for cycling one truckload of solution is still 50 min, the same as at the peak load condition, so the total transportation time of the truck can be approximated as the equivalent full (peak) load hours of the absorption chiller.

APPENDIX D. PIPELINE TRANSPORTATION CALCULATION

D-1. PIPE SIZE AND COST

The pipe size (diameter) is calculated based on the required mass flow rate of the working fluid for satisfying the peak cooling load. From the Houston case study, the total chiller size is 871 ton (3,063 kW). The solution energy density is 0.1 kWh_{clg}/kg weak solution; therefore, the peak hourly consumption rate of the weak solution is

$$m_{WS} = \frac{Q_{evap}}{\frac{Q_{cool}}{M_{WS}}} = \frac{Q_{evap} * C_{SS}}{(C_{SS} - C_{WS}) * h_{fg}} = 31,672 \text{ [kg/hr]}$$

With the density (ρ) of 58% LiBr/H₂O solution, which is around 1,600kg/m³, the peak mass flow rate is converted to peak volumetric flow rate as follows:

$$M_{pipe} = \frac{\text{mass flow rate}}{\text{density}} = 19.8 \text{ [m}^3\text{/hr]} = 87.1 \text{ [gpm]}$$

Typically, the minimum pipe diameter for a 87.1 gpm flow rate is 3 in. (GHC 2001).

Several types of pipes made with different materials can be used to transport LiBr/H₂O solution. Since the LiBr/H₂O solution is corrosive to metal, only plastic pipes are considered, including polyvinyl chloride (PVC), chlorinated polyvinyl chloride (CPVC), and high-density polyethylene (HDPE).

To circulate the working fluid over a 10-mile distance between the geothermal site and the building, the total length of pipes is 105,600 ft. The prices of 3 in. diameter PVC, CPVC, and HDPE pipes obtained from RSMMeans 2010 are listed in Table D-1 along with the total costs of the 10-mile long, two-way pipeline.

Table D-1. Cost of pipes made with different materials (Reed Construction 2010)

Material	Price (\$/ft)	Total cost (\$)	Specifications
PVC	28	2,956,800	SDR21, 200psi
CPVC	37.5	3,960,000	socket joint
HDPE	1.32	357,500	Single wall DR11 + \$21 per 40' welding + excavation ^a

^a DR stands for “diameter ratio”; it is the ratio of the pipe diameter to the pipe wall thickness.

As shown in Table D-1, the price of HDPE pipe is the lowest among the three plastic pipes. Even considering the labor cost for welding the joints and excavating trenches, the total cost of pipeline using HDPE is about an order lower than other options.

D-2. PUMPING COST

D-2.1 Pressure drop

As calculated in section D-1, the peak volumetric flow rate (q) of the working fluid (i.e., the weak solution) is $19.8\text{m}^3/\text{h}$ (87.1 gpm), and the selected pipe diameter (d) is 3 in. (0.0762 m). Thus the velocity of the solution in the pipe (u) is 1.21m/s. For the 10-mile distance scenario, the total length of one pipe (L) is 52,800 ft (16,093 m). For HDPE pipe, the roughness (k) is 0.0015 mm. The dynamic viscosity (μ) of the weak (58%) LiBr/H₂O solution at 30°C is $6.3e^{-3}$ Pa•s (Martin and Berntsson 1994).

Based on parameters given above, the Reynolds number is calculated as

$$Re = \frac{\rho u L}{\mu} = \frac{1600 * 1.21 * 0.0762}{6.3e^{-3}} = 23,416$$

The friction coefficient (λ) is calculated with the Colebrook–White equation, and the result is 0.0249.

$$\frac{1}{\lambda^{\frac{1}{2}}} = -2 * \log \left[\frac{2.51}{Re * \lambda^{\frac{1}{2}}} + \frac{k}{3.72d} \right]$$

The pressure loss along a 10-mile long HDPE pipe is calculated as

$$\Delta p = \lambda * \frac{L}{d} * \left(\rho * \frac{u^2}{2} \right) = 0.0249 * \frac{16093}{0.0762} * \frac{\left(1,600 * \left(\frac{1.21^2}{2} \right) \right)}{1000} = 6,122.5 \text{ kPa} = 624.7 \text{ mH}_2\text{O} = 888 \text{ psi}$$

D-2.2 Pumping power and cost

Hydraulic pumping power can be calculated given the pressure drop:

$$P_h = \frac{q * \rho * g * h}{3.6e6} = \frac{19.8 * 1,600 * 9.8 * 624.7}{3.6e6} = 53.9 \text{ kW} = 72.2 \text{ hp}$$

Assuming pumping efficiency (η) is 0.6, the shaft power of the motor is

$$P_s = \frac{P_h}{\eta} = 89.9 \text{ kW} = 120.4 \text{ hp}$$

The annual electricity consumption of circulation pumps in the pipeline can be estimated using the equivalent full-load hour (EFLH):

$$Ele_{pipe_{pump}} = P_s * EFLH = 198,589 \text{ kWh}$$

For the two-pipe pipeline system, the annual pumping cost in Houston area is

$$Cost_{pipe_{pumping}} = UR * Ele_{pipe_{pump}} = \$40,500$$

HDPE pipe (DR=11) at 100°F (37°C) has a pressure rating of 125 psi¹⁵. To ensure the maximum pressure at the HDPE pipe is lower than its limit, 16 identical pumps are installed in series at evenly divided distance along the pipeline. According to RSMMeans 2010, the installed cost of a circulation pump with 90 GPM nominal flow rate is \$6,750. Therefore, the total cost of the 16 circulation pumps in the pipeline is \$108,000.

The capital costs to build and maintain pump stations along the pipeline are not included in this cost estimation.

D-3 SOLUTION COST

In order to achieve a continuous operation, the pipeline needs to be filled with working fluid. The total amount of needed working fluid is calculated given the diameter and total length of the pipes and it is 234, 735 kg. Given the price of 55% LiBr/H₂O solution is \$3.55/kg, the total cost of LiBr/H₂O solution is \$833,310.

REFERENCES

- GHC (Geo-Heat Center). 2001. "Well Pumps and Piping," *GHC Bulletin*, September 2001.
- Martin, J., Berntsson, T. 1994. "Viscosity and density of aqueous solutions of LiBr, LiCl, ZnBr₂, CaCl₂, and LiNO₃. 1. Single Salt Solutions," *J. Chem. Eng. Data* 1994, 39, 68–72.
- Reed Construction. 2010. "RS Means Mechanical Cost Data 2010." Kingston, MA.

¹⁵ Source: <https://plasticpipe.org/pdf/tn-27-faq-hdpe-water-transmission.pdf>

